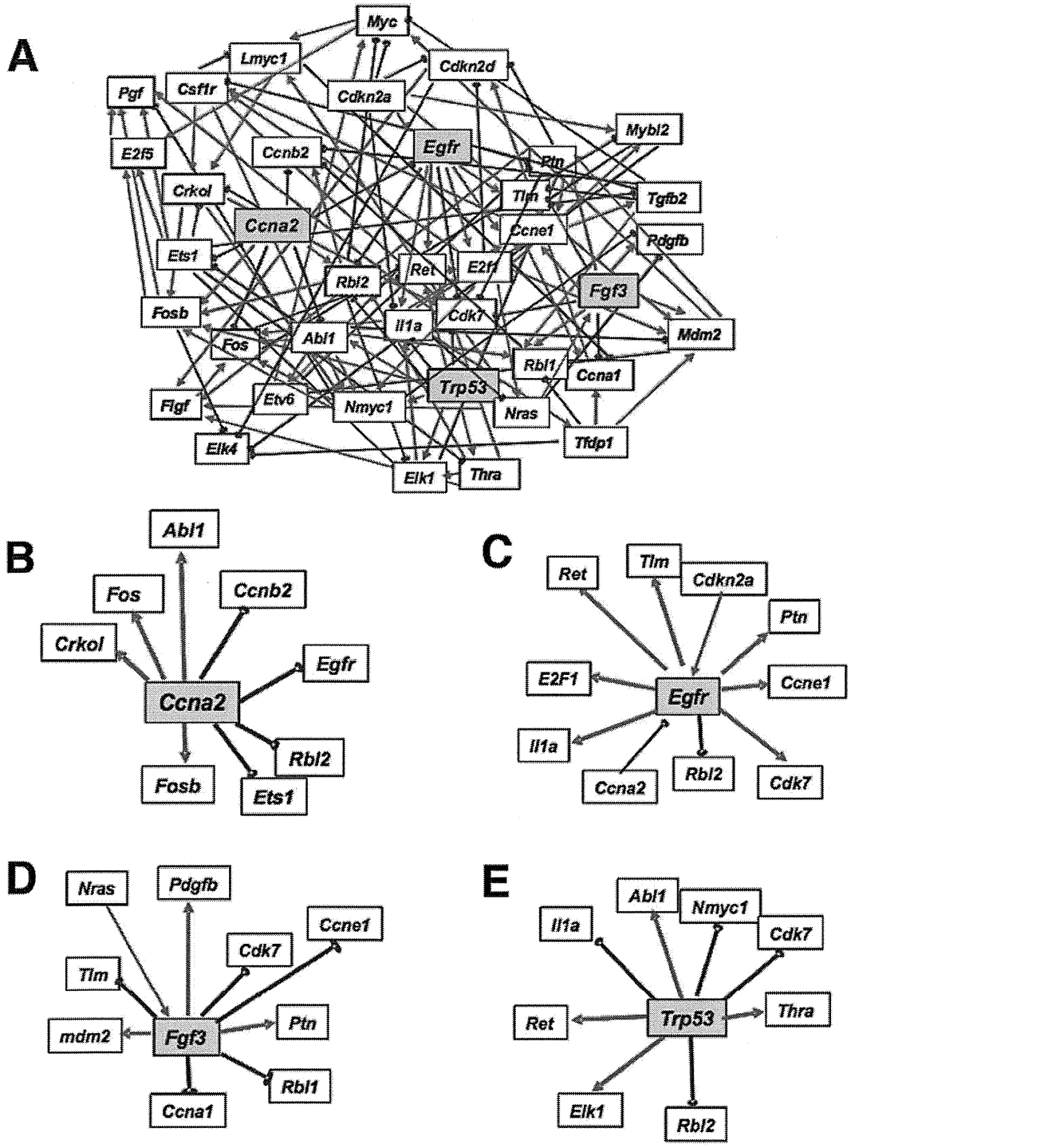

Fig. (3). Networks identified for the G1/S course data (**A**) and the isolated linkages associated with nodal genes Ccna2 (**B**), Egfr (**C**), Fgf3 (**D**) and Trp53 (**E**). Red arrows indicate linkages associated with upregulation and blue arrows indicate linkages associated with downregulation for any two genes within the network. Bold lines indicate linkages with nodal genes.

In the network found for the G1/S start data subset in hydroxyurea treated MEFs, the structure was observed to be more complicated and have no obvious central nodes. In this network, the number of connections from *Cdk7* and *Cdkn2a* to other genes was greatly decreased, whereas the connections from *Ccna2*, *Egfr*, *Fgf3*, *Trp53*, *Nmyc1*, *Ptn*, and *Rbl2* were increased (Fig. **3A**). These changes suggested that growth factors, such as *Egfr*, *Fgf3*, and *Ptn*, and proliferation regulators, such as Ccna2, Trp53, and Rbl2, have more prominent roles during S phase progression (Fig. **3B-E**). From these data, it becomes obvious that the gene networks which regulate the progression of the cell cycle completely differ between the G0-G1 and G1-S transitions.

Table 3. Number of Linkages Between the 39 Selected Genes Related to Cell Cycle Control in MEFs

Gene Name	G0 Course			G1/S Course		
	Outward	Inward	Total	Outward	Inward	Total
Abl1	8	1	9	6	2	8
Ccna1	1	2	3	1	4	5
Ccna2	0	4	4	8	0	8
Ccnb2	2	5	7	0	4	4
Ccne1	0	2	2	3	5	8
Crkol	0	4	4	1	4	5
Csf1r	5	0	5	4	3	7
E2f5	2	3	5	1	3	4
Egfr	4	4	8	8	2	10
Elk1	0	3	3	2	4	6
Elk4	1	5	6	0	4	4
Ets1	6	3	9	6	2	8
Etv6	3	4	7	3	2	5
Fgf3	6	0	6	8	1	9
Figf	1	5	6	1	4	5
Fos	1	1	2	2	5	7
Fosb	5	4	9	3	5	8
Il1a	2	5	7	5	4	9
Lmyc1	3	1	4	2	3	5
Mybl2	1	4	5	2	3	5
Myc	3	1	4	2	5	7
Nmyc1	1	4	5	4	4	8
Nras	2	3	5	5	2	7
Pdgfb	3	0	3	0	3	3
Pgf	1	5	6	0	5	5
Ptn	1	3	4	4	5	9
Ret	1	4	5	0	5	5
Tfdp1	2	5	7	4	1	5
Tgfb2	4	3	7	5	2	7
Thra	3	3	6	4	2	6
Tlm	2	5	7	0	4	4
E2f1	6	0	6	7	3	10
Trp53	4	4	8	8	0	8
Mdm2	4	3	7	3	5	8
Cdkn2a	13	1	14	6	0	6
Cdk7	10	1	11	1	5	6
Rbl1	3	4	7	1	4	5
Rbl2	1	4	5	5	4	9
Cdkn2d	2	4	6	2	4	6

Name abbreviations of the genes analyzed in this study are as listed in Table 2.

Verification of the Quantified Network

Further analyses were conducted to determine the statistical significance of the linkages between our identified genes. To find the most prominent linkages between genes of the network from Cdk7 and of the network from Trp53, the G0 course dataset and the G1/S course dataset obtained from MEFs treated with serum starvation or hydroxyurea were used, respectively. This analysis method can predict both the strength of the relationships between genes and the posterior distribution of parameters in the log-linear model [22, 23]. Of the 10 genes associated with *Cdk7*, 9 had some posterior densities that did not include 0, suggesting very significant associations (Table **4**). Only Il1a included 0 in the posterior density, with 18% of the distribution above zero and 82% below. This finding suggested a statistically marginal down-regulation. Fig. (**4**) illustrated the distribution for a strong down-regulation (*Cdk7* → *Nras*) and for a weak down-regulation (*Cdk7* → *Il1a*). A negative association between *Nras* and *Cdk7* has been reported previously [28], suggesting that the method we employed in our present analyses can extract negative relationships between two genes using simple microarray data.

Table 4. Summary of the Results from the MCMC Analyses

Parent	Target	Mean	Std.	Percent <0
G0 Network				
Cdk7	Ccna2	-6.0037	0.0718	0
	Egfr	-2.5725	0.0265	0
	Etv6	2.0637	0.0279	0
	Figf	1.4832	0.0022	0
	Ll1a	-1.0015	1.0882	17.9
	Mybl2	-2.8674	0.0141	0
	Nmyc1	-0.712	0.0064	0
	Nras	-2.8768	0.0626	0
	Rgf	6.7274	0.0059	0
	Rbl1	1.9701	0.0065	0
G1 Network				
P53	Abl1	0.9456	0.4592	0.0225
	Cdk7	-3.7324	0.0008	0
	Elk1	6.7449	1.3828	0.004
	Ll1a	-1.5102	0.0721	0
	Nmyc1	6.1901	0.0417	0
	Rbl1	-6.6934	0.3521	0
	Ret	1.7052	2.7057	25.7

For G0 data, MCMC sampling was performed 140,000 times and the mean, standard deviation (Std.) and percentage below zero were assessed from the last 70,000 samplings. If the number was negative, only the samples above zero were counted. For G1 data, MCMC sampling was performed 300,000 times and the mean, Std., and percentage below zero were assessed from the last 150,000 samplings.

In the G1/S network, *Trp53* suppressed the expression of *Cdk7* and *Rbl2*, and stimulated that of *Abl1*, *Il1a*, *Nmyc*, *Elk1*, *Ret* and *Thra* (Fig. **3E**). *Trp53* has previously been

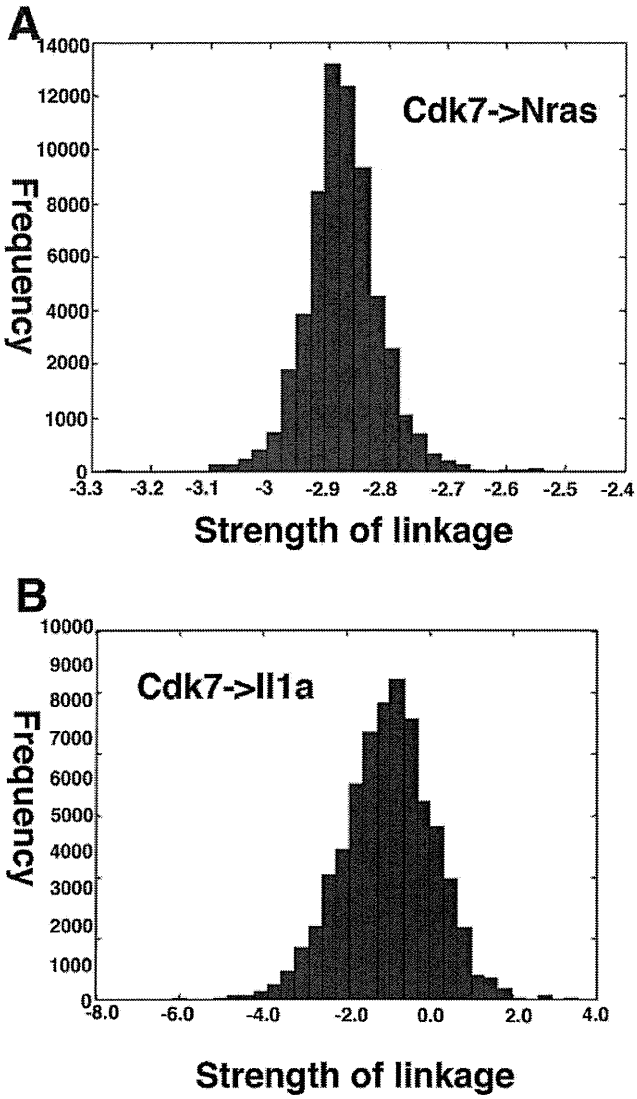

Fig. (4). (**A**, **B**) Frequency histograms approximating the posterior distributions for linkages from Cdk7 to Nras (a statistically significant downregulation) and Cdk7 to Il1a (marginally significant downregulation). Histograms were derived by Bayesian analysis of the gene interaction network shown in Fig. (**2C**) using 70,000 out of 140,000 Markov-Chain Monte Carlo samples and prior distributions as shown in Table **4**.

shown to negatively regulate cyclinD/CDK4, cyclinD/CDK6, cyclinB/cdk2, and cyclinA/cdk2 through the activation of p21 in normal cells. CyclinD/CDK4/6 on the other hand activates phosphorylated RB (pRb) which leads to the activation of E2F, which in turn negatively regulates p53 through $p19^{ARF}$ activation and MDM2 suppression [1, 29]. The interaction between p53 and c-Abl is known to play a critical role in the cell growth and G1 arrest response to DNA damage under normal conditions [30]. It has been reported that CDK7 phosphorylates other CDKs, which is an essential step for their activation [31] and that a direct involvement of p53 in triggering growth arrest by its interaction with the CDK activating kinase complex [32]. These reports and our predictive network suggest therefore that CDK7 is essential for mitosis.

Detection of Gene Networks Using a Recombinant Mouse CDK7 Retrovirus System

Our cell cycle network data indicated that CDK7 activation negatively regulates the expression of *Egfr* and *Nmyc1* in MEFs. To validate this observation, we introduced mouse CDK7 into these cells using a recombinant retrovirus system to evaluate negative regulation of CDK7 against EGFR and N-MYC. The titer of the retrovirus obtained from PT67 producer cells was 4.0 X 10^9 virus copies/ml for the LXIN empty vector and 5.4 X 10^9 virus copies/ml for the CDK7 recombinant retrovirus. The hemagglutinin (HA) protein tag was added to the carboxyl terminus of recombinant CDK7 so that we could distinguish the recombinant protein from its endogenous counterpart.

As shown in Fig. (**5**), western blot detection with a HA antibody revealed the expression of recombinant CDK7 protein in infected MEF cells. Increased levels of total CDK7 protein (endogenous plus recombinant CDK7) was also confirmed by immunoblotting with a CDK7 antibody (Fig. **5A**). The EGFR, N-MYC1 and c-FOS protein levels detected by western blot were decreased in MEF cells infected with the CDK7-expressing retrovirus when compared with the control cells (Fig. **5A**). c-FOS was used as control because there was no direct linkage between CDK7 and c-FOS (see Fig. **2A**). The average levels of EGFR and N-MYC1 from three separate experiments are shown in Fig. (**5B**). Decreased EGFR and N-MYC1 but not c-FOS protein levels indicated that the exogenous introduction of CDK7 negatively influenced their expression. From these results, we concluded that one part of our newly detected cell cycle network had been validated.

DISCUSSION

Gene set enrichment is one means of providing reliable information about specific basic biological processes and has been the most widely used gene-set analysis method to date [33-36]. Directed graphical models known as Bayesian networks, and the MCMC method of determining network inference, have been show to be promising approaches to obtaining new information about gene networks in various tissues and cells.

In our current study, we adopted an approach based on a systematic analysis of gene expression data to define a gene regulatory network and new putative CDK7 functions were identified by quantifying the dynamics of the gene regulatory networks for cell cycle control in MEF cells. A previous study has suggested that a TFIIH complex containing CDK7 is responsible for the phosphorylation of CDK2 and CDK4, both of which are crucial contributors to the G1/S cell cycle transition in human and mouse cells [37]. One of the TFIIH components critically regulates the CAK activity of CDK7 during mitotic progression, suggesting that mitotic silencing of basal transcription is important to the *Drosophila* cell cycle [38]. The previous study indicated that the phosphorylation of CDK7 cause the inhibition of TFIIH-associated kinase and transcriptional activity [39]. Although we do not have any data about the phospholylation status of introduced recombinant CDK7 protein, there is a possibility that the extra amount of CDK7 protein resulted in the reduced transcriptional activity of TFIIH. The gene networks

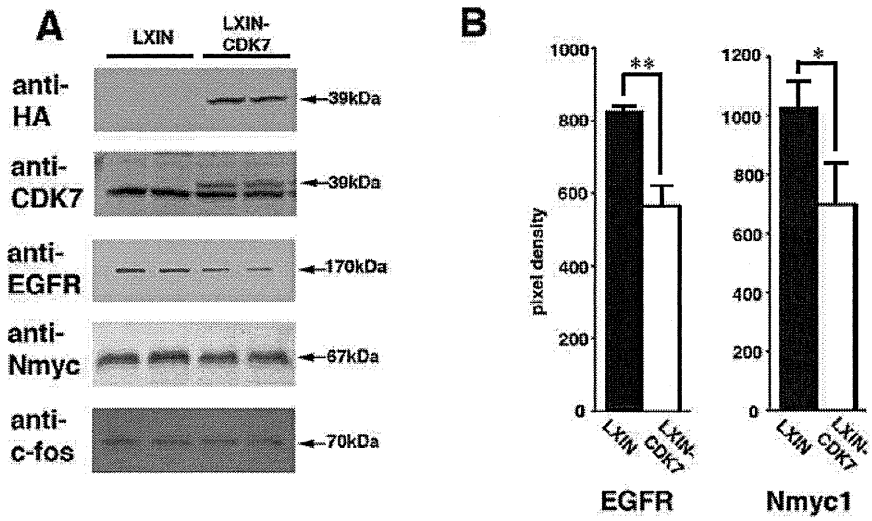

Fig. (5). Experimental verification of detected gene network from Cdk7 to EGFR and N-myc1 using a recombinant retrovirus expression system. (**A**) The protein levels of exogenous Cdk7 (HA), total Cdk7 (Cdk7), EGFR, and N-myc1 were detected by western blotting. Representative blots obtained from two independent samples are shown in the figure. (**B**) EGFR and N-myc1 protein levels were quantitatively analyzed. Data are the average plus standard deviation of 6 western blots from two independent samples for each group. *, $P < 0.05$; **, $P < 0.01$.

found in this study have to be further evaluated in terms of whether they are based on direct or indirect interactions, however, this is to our knowledge the first report showing the importance of CDK7 associated networks for the progression from G0 to G1.

We also analyzed gene networks associated with S phase and M phase, in addition to the progression from G0 to G1, which focused in our current linkage analysis. Several central nodes were detected but their networks will need to be further evaluated experimentally, as shown for CDK7 in this study. We thus reveal that the qualitative algorithm based on Bayesian networks is a useful tool for detecting gene networks that function at specific phases of the cell cycle. Our results indicate that CDK7 negatively regulates EGFR and N-myc expression to control G1 entry. When the MEF cells do enter G1 from G0, the expression of *Cdk7* is suppressed, resulting in the increased expression of the *Egfr and N-myc* genes and protein products. EGFR is known act as a growth factor receptor, and activated EGFR is known to promote cell cycle progression through the G1-related Cyclin complex. N-myc is also known to stimulate cell proliferation and CDK7 thus appears to act as a negative regulator of cell proliferation and cell cycle progression in mammalian cells.

Although the CAK activation at the G1/S phase transition promotes mitotic progression, the relationship between Cdk7 and Egfr was observed at the G0/G1 phase but not the G1/S phase in our case. When we looked for the relationship between two genes at the database GEO (http://www.ncbi.nlm.nih.gov/sites/GDSbrowser) for confirming our data, the relationships are reversal at the early stage after several treatments of serum starvation, cat or Camptothecin. This public evidences can support our data, implicating that CDK7 regulates EGFR expression levels according to the type of cell cycle stage.

Our study detected the gene networks from CDK7 to the downstream. As the next step for the study, these inhibitory effects would be needed to analyze from the viewpoint of kinetics. The kinetics study would explore how fast the transcriptional inhibition reaches to the equilibrium in the process of the cell cycle. The time course analysis with the efficient inducible expression system of recombinant CDK7 would be required to get these data.

Whereas our overall approach in this study was based upon a specific set of tools, other tools could be used to obtain similar findings. Gene ontology was used to select specific genes to consider when defining the network. Other classification methods however, such as clustering, could have also been used to select a specific gene group. Sequence/structure analysis of transcription factors in order to verify gene nodes could be replaced by analyses of protein structure, protein-protein interactions, or protein-DNA interactions. The log-linear mathematical model used to quantify gene interactions could easily be replaced by mechanism-based dynamic models if the data could support more parameters. However, the simplicity of the model used in this analysis has the advantage of providing rapid identification of gene relationships that are helpful in elucidating the structure and dynamics of the gene network using only gene expression profiles. With only one parameter in the model for each gene-gene relationship, one can more easily visualize and understand complex network relationships.

We validated part of our predicted network with a retrovirus CDK7 expression system. The exogenous introduction of mouse CDK7 into MEF cells caused a decrease in the protein levels for EGFR and N-MYC1. These findings provided supporting evidence for the validity of our detected gene network. The molecular weight of the retroviral CDK7 was slightly higher than the endogenous

protein in mouse MEF cells. According to the Genbank database, there is an alternative splice site at the position of exon 6 in CDK7 (accession number: NMV009874.3). Although our cloned CDK7 is the most common form (346aa, 38.9kDa, accession number: NMV009874), and was mainly used in previous functional studies, there is a possibility that endogenous CDK7 expressed in MEF cells is a short form of this protein that arises through the alternative splicing of exon 6. We predict that there is no functional difference between the short form of CDK7 and our recombinant version, since the binding site of MAT7 and phosphorylation sites are present in both forms.

To further test the negative regulatory relationship between CDK7 and EGFR or N-MYC, we attempted to knockdown endogenous CDK7 using a siRNA approach and also a Cre-loxP mediated conditional expression system. However, neither approach was successful in the MEF cells due to a low transfection efficiency for siRNA and the cell toxicity of the adenovirus which expresses the Cre recombinase.

Another important factor to consider is the condition of the MEFs. We used cells that were not immortalized, which allowed us to investigate gene network dynamics in a normal cell context. However, such cells are severely limited in their replicative capacity, resulting in a limited number of applicable approaches for genetic manipulation. Since the inactivation of both p16 and p53 has previously been reported to be essential for the immortalization of MEFs, it is almost certain that the entire cell cycle network would be severely affected by the immortalization process.

An important objective in Bayesian network learning is to infer the network topology. We used 39 genes based on MAP criterion in this study. Even with 39 genes, the topology space is 2^39. However, it is difficult (virtually impossible) to conclude that the optimized network is the best one without doing all possible topologies, an impossibility for 2^{39} topologies. Therefore, a search algorithm, described with step-by-step instructions in the previous work [21], was used to obtain a network topology. Also in the previous work [21], a series of simulation studies were undertaken to address the operating characteristics of the algorithm and to determine the conditions under which it would fail. The analysis used a simple log-linear model to infer linkages in the network. The approach used has advantages and disadvantages over other approaches. The major advantage is a compact parameter space using the minimum number of parameters to infer the network that allows us to use a single parameter to infer the strength of a linkage. This also reflects on the major disadvantage in that is not possible to use this model to describe the dynamics of the interactions *per se* as such a mechanistic model would require more complex biomathematical descriptions of each linkage and considerably more data. That said simple linear models have been a mainstay of descriptive statistical evaluations of biological data for decades. In this case, they allow us to test the hypothesis of no linkage between genes against the alternative of a proportionate change on a log-scale and infer linkage.

The analysis tool used here is able to find genes that appear to be positively or negatively correlated as the gene expression patterns change over time. If a gene is only changed at one time, say 6 hours, and its target genes are only altered at a different time, say 12 hours, this algorithm would be unlikely to identify the linkage. A dynamic model, describing the patterns over time in a more mechanistic fashion, might locate such a linkage, although it might still be very difficult. For the data being examined here, it is more likely that the dynamic changes in gene expression occur gradually throughout the course of the experiment (18-24 hours) resulting in correlations through time that can be observed in our simple linear model.

In summary, the results of our network analyses have raised a number of new possibilities concerning the roles of numerous genes in the regulation of the murine cell cycle. The limitations of these analyses (use of only microarray data, a simple log-linear model, and promoter region sequences) preclude a stronger interpretation of the results. However, as additional data are obtained in future studies that address the hypothetical linkages identified by our findings, it should be possible to bring them formally into an improved analysis and critically evaluate each linkage in greater detail. This is the overall goal of cancer systems biology and the general approach presented here should form the basis for future attempts at system-wide analyses of biological function.

ACKNOWLEDGEMENTS

We thank Leping Li, Delong Liu, Rick Paules, David Umbach, Scott Auerbach and Ben Van Houten (NIH/NIEHS) for their comments on this work, and J. R. Nevins and S. Ishida for kindly providing the original dataset. This research was supported in part by the National Institute of Environmental Health Sciences.

SUPPLEMENTAL MATERIALS

This article also contain supplementary material and it can be viewed at publisher's website along with the article.

REFERENCES

[1] Sears RC, Nevins JR. Signaling networks that link cell proliferation and cell fate. J Biol Chem 2002; 277: 11617-20.

[2] Stillman B. Cell cycle control of DNA replication. Science 1996; 274: 1659-64.

[3] Cho RJ, Huang M, Campbell MJ, *et al.* Transcriptional regulation and function during the human cell cycle. Nat Genet 2001; 27: 48-54.

[4] Ishida S, Huang E, Zuzan H, *et al.* Role for E2F in control of both DNA replication and mitotic functions as revealed from DNA microarray analysis. Mol Cell Biol 2001; 21: 4684-99.

[5] Iyer VR, Eisen MB, Ross DT, *et al.* The transcriptional program in the response of human fibroblasts to serum. Science 1999; 283: 83-7.

[6] Haller F, Gunawan B, von Heydebreck A, *et al.* Prognostic role of E2F1 and members of the CDKN2A network in gastrointestinal stromal tumors. Clin Cancer Res 2005; 11: 6589-97.

[7] Katoh Y, Katoh M. Identification and characterization of DISP3 gene *in silico*. Int J Oncol 2005; 26: 551-6.

[8] Tonon G. From oncogene to network addiction: the new frontier of cancer genomics and therapeutics. Future Oncol 2008; 4: 569-77.

[9] Emmert-Streib F, Dehmer M. Predicting cell cycle regulated genes by causal interactions. PLoS One 2009; 4: e6633.

[10] Margolin AA, Califano A. Theory and limitations of genetic network inference from microarray data. Ann N Y Acad Sci 2007; 1115: 51-72.

[11] Djebbari A and Quackenbush J: Seeded Bayesian Networks: constructing genetic networks from microarray data. BMC Syst Biol 2: 57, 2008.

[12] Gevaert O, De Smet F, Kirk E, *et al.* Predicting the outcome of pregnancies of unknown location: Bayesian networks with expert prior information compared to logistic regression. Hum Reprod 2006; 21: 1824-31.

[13] Nakayama KI, Nakayama K. Ubiquitin ligases: cell-cycle control and cancer. Nat Rev Cancer 2006; 6: 369-81.

[14] Nourse J, Firpo E, Flanagan WM, *et al.* Interleukin-2-mediated elimination of the p27Kip1 cyclin-dependent kinase inhibitor prevented by rapamycin. Nature 1994; 372: 570-3.

[15] Reynisdottir I, Polyak K, Iavarone A, *et al.* Kip/Cip and Ink4 Cdk inhibitors cooperate to induce cell cycle arrest in response to TGF-beta. Genes Dev 1995; 9: 1831-45.

[16] Susaki E, Nakayama K, Nakayama KI. Cyclin D2 translocates p27 out of the nucleus and promotes its degradation at the G0-G1 transition. Mol Cell Biol 2007; 27: 4626-40.

[17] Susaki E, Nakayama KI. Multiple mechanisms for p27(Kip1) translocation and degradation. Cell Cycle 2007; 6: 3015-20.

[18] Tanaka A, Muto S, Konno M, *et al.* A new IkappaB kinase beta inhibitor prevents human breast cancer progression through negative regulation of cell cycle transition. Cancer Res 2006; 66: 419-26.

[19] Matsumoto G, Namekawa J, Muta M, *et al.* Targeting of nuclear factor kappaB Pathways by dehydroxymethylepoxyquinomicin, a novel inhibitor of breast carcinomas: antitumor and antiangiogenic potential *in vivo*. Clin Cancer Res 2005; 11: 1287-93.

[20] Elangovan S, Hsieh TC, Wu JM. Growth inhibition of human MDA-mB-231 breast cancer cells by delta-tocotrienol is associated with loss of cyclin D1/CDK4 expression and accompanying changes in the state of phosphorylation of the retinoblastoma tumor suppressor gene product. Anticancer Res 2008; 28: 2641-7.

[21] Yamanaka T, Toyoshiba H, Sone H, *et al.* The TAO-Gen algorithm for identifying gene interaction networks with application to SOS repair in E. coli. Environ Health Perspect 2004; 112: 1614-21.

[22] Toyoshiba H, Sone H, Yamanaka T, *et al.* Gene interaction network analysis suggests differences between high and low doses of acetaminophen. Toxicol Appl Pharmacol 2006; 215: 306-16.

[23] Toyoshiba H, Yamanaka T, Sone H, *et al.* Gene interaction network suggests dioxin induces a significant linkage between aryl hydrocarbon receptor and retinoic acid receptor beta. Environ Health Perspect 2004; 112: 1217-24.

[24] Dahlquist KD, Salomonis N, Vranizan K, *et al.* GenMAPP, a new tool for viewing and analyzing microarray data on biological pathways. Nat Genet 2002; 31: 19-20.

[25] Fukuda T, Mishina Y, Walker MP, *et al.* Conditional transgenic system for mouse aurora a kinase: degradation by the ubiquitin proteasome pathway controls the level of the transgenic protein. Mol Cell Biol 2005; 25: 5270-81.

[26] Nigg EA. Cyclin-dependent kinase 7: at the cross-roads of transcription, DNA repair and cell cycle control? Curr Opin Cell Biol 1996; 8: 312-7.

[27] Schulze A, Zerfass K, Spitkovsky D, *et al.* Activation of the E2F transcription factor by cyclin D1 is blocked by p16INK4, the product of the putative tumor suppressor gene MTS1. Oncogene 1994; 9: 3475-82.

[28] Abdellatif M, Packer SE, Michael LH, *et al.* A Ras-dependent pathway regulates RNA polymerase II phosphorylation in cardiac myocytes: implications for cardiac hypertrophy. Mol Cell Biol 1998; 18: 6729-36.

[29] Ball KL p21: Structure and Functions Associated with Cyclin-cdk Binding. In: L Meijer, Guidet, S., Philippe, M. (ed.), Progress in cell cycle research: Plenum press, New York, Vol. 3, pp. 125. 1997.

[30] Sionov RV, Coen S, Goldberg Z, *et al.* c-Abl regulates p53 levels under normal and stress conditions by preventing its nuclear export and ubiquitination. Mol Cell Biol 2001; 21: 5869-78.

[31] Larochelle S, Pandur J, Fisher RP, *et al.* Cdk7 is essential for mitosis and for *in vivo* Cdk-activating kinase activity. Genes Dev 1998;12: 370-81.

[32] Schneider E, Montenarh M, Wagner P. Regulation of CAK kinase activity by p53. Oncogene 1998; 17: 2733-41.

[33] Subramanian A, Tamayo P, Mootha VK, *et al.* Gene set enrichment analysis: a knowledge-based approach for interpreting genome-wide expression profiles. Proc Natl Acad Sci U S A 2005; 102: 15545-50.

[34] Goeman JJ, Buhlmann P. Analyzing gene expression data in terms of gene sets: methodological issues. Bioinformatics 2007; 23: 980-7.

[35] Mootha VK, Lindgren CM, Eriksson KF, *et al.* PGC-1alpha-responsive genes involved in oxidative phosphorylation are coordinately downregulated in human diabetes. Nat Genet 2003; 34: 267-73.

[36] Toyoshiba H, Sawada H, Naeshiro I, *et al.* Similar compounds searching system by using the gene expression microarray database. Toxicol Lett 2008.

[37] Watanabe Y, Fujimoto H, Watanabe T, *et al.* Modulation of TFIIH-associated kinase activity by complex formation and its relationship with CTD phosphorylation of RNA polymerase II. Genes Cells 2000; 5: 407-23.

[38] Chen J, Larochelle S, Li X, *et al.* Xpd/Ercc2 regulates CAK activity and mitotic progression. Nature 2003; 424: 228-32.

[39] Akoulitchev S, Reinberg D. The molecular mechanism of mitotic inhibition of TFIIH is mediated by phosphorylation of CDK7. Genes Dev 1998; 12: 3541-50.

Received: May 11, 2009 Revised: February 1, 2010 Accepted: March 1, 2010

Genes and Environment, Vol. 33, No. 2 pp. 43–49 (2011)

Review

Perinatal Exposure to Environmental Chemicals Induces Epigenomic Changes in Offspring

Seiichiroh Ohsako[1]

Division of Environmental Health Sciences, Center for Disease Biology and Integrative Medicine, Graduate School and Faculty of Medicine, The University of Tokyo, Tokyo, Japan

(Received February 21, 2011; Revised March 10, 2011; Accepted March 10, 2011)

Many researchers propose that invisible internal alterations that occur through exposure to environmental factors during fetal or neonatal stages affect the risk of cancer, hypertension, and diabetes after maturation. Barker's hypothesis, which states that reduced fetal growth is strongly associated with metabolic syndromes including cardiovascular disease and diabetes, has now been widely accepted and expanded into the Developmental Origins of Health and Disease (DOHaD). Potential molecular mechanisms underlying this phenomenon include the alteration and persistence of epigenomic programming. Clear biochemical evidence has not yet been obtained in human studies; however, in laboratory animals, the fetal environment including physical and chemical factors altered epigenomic states such as DNA methylation and histone modification, and persistent changes affected specific gene expression regulation, resulting in disease susceptibility. Furthermore, in recent studies, environmental chemical exposure during pregnancy altered sperm DNA methylation patterns of male offspring, and the altered status and resulting phenotypes were inherited in the next generation. Challenging and eccentric studies focusing on epigenetic transgenerational effects are currently being conducted to demonstrate the existence of Lamarckian inheritance.

Key words: epigenetics, environmental chemical, DOHaD, acquired characteristics

Introduction

Recently, several researchers have proposed that invisible alterations that occur as a result of exposure to environmental factors during fetal or immature stages influence the risk of cancer, hypertension, and diabetes in adulthood. The molecular bases for disease susceptibilities are linked to epigenetics (1–5). Various environmental factors surrounding pregnant mothers and infants could be potential stimuli for epigenome alternation. For example, nutrient changes, exposure to environmental chemicals, and physical stresses such as insufficient care can alter the epigenome; thus, concern regarding chemicals that affect the health of the next generation has recently increased (6–9). In this review, several studies conducted on animals are presented to summarize the evidence that the fetal and neonatal environment can influence epigenomic modifications retained in later stages of life.

Epigenome Features and Mechanism of Their Structural Inheritance

In the field of epigenetic research, a considerable amount of attention has been paid to DNA methylation and histone modification because these processes are the most important epigenomic features. Variations in the amino acid acetylation/methylation status of histone octamers in the nucleosome of specific regions of chromatin and changes in DNA cytosine methylation patterns can be inherited by daughter cells after replication and cell division. Therefore, chromatin modification patterns are considered genetic information (epigenetic information or memory) (10).

DNA methylation typically occurs at CpG sites, which are 5′-CG-3′ dinucleotide sequences. Cytosine nucleotides of CpG are not methylated in newly synthesized DNA strands; thus, this double stranded state is called hemi-methylated DNA. Immediately after DNA replication, hemi-methylated DNA is recognized by Np95 (UHRF1) (11), which is a component of the replication factory complex. This complex contains proliferating cell nuclear antigen (PCNA) and DNA methyltransferase 1 (DNMT1), which transfers a methyl group to the 5 position of unmethylated cytosine in the newly synthesized opposite DNA strand (12,13). By this simple mechanism, information with methyl-CpG patterns (methylation status) is maintained in the nucleus of the daughter cell. CpG sites occur at a relatively low frequency in the genome. Because methyl-CpG sites are more susceptible to mutation and are lost over time,

[1]Correspondence to: Seiichiroh Ohsako, Division of Environmental Health Sciences, Center for Disease Biology and Integrative Medicine, Graduate School of Medicine, The University of Tokyo, 7-3-1 Hongo, Bunkyo-ku, Tokyo 113-8654, Japan. Tel: +81-3-5841-1432, Fax: +81-3-5841-1434, E-mail: ohsako@m.u-tokyo.ac.jp

CpG clusters or CpG islands are located on a specific region of the genome, i.e., gene promoter and exon 1. CpG methylation negatively regulates gene expression because transcription factors cannot bind methyl-CpG containing elements (14). Thereby, CpG islands of cell type specific regulatory genes are methylated followed by further chromatin modification. This chromatin remodeling including CpG methylation is highly correlated with cellular transformation and differentiation (15,16).

A histone octamer composed of one H2A, one H2B, two H3, and two H4 proteins is one unit of the nucleosome. Acetylation and methylation of acidic amino acid residues (lysine and arginine) in the amino-terminals of histone H3 and H4 are major epigenetic marks. In addition, phosphorylation, ubiquitination, sumoylation, ADP-ribosylation, and biotinylation are other chemical modifications of the histone tail (17). Histone acetylation and methylation are attuned to transcription activation and chromatin inactivation, respectively. Patterns of the covalent modifications of histone tails are extremely varied due to the number of modifiable amino acids and the possible combinations of substitution. Code information other than nucleotide sequences was advocated as the histone-code hypothesis; however, this theory is currently disregarded (18). Nevertheless, these histone-based modification patterns must influence region specific chromatin structure, resulting in differences in the level of gene expression. Many mechanistic models have been constructed to explain how histone modification patterns are inherited by daughter cells. In particular, a random distribution model is shown in Fig. 1 (19). On the newly synthesized DNA, parental histone H3–H4 tetramers are reused for the formation of the nucleosome of daughter chromatin. At the same time, newly synthesized histone H3–H4 tetramers are incorporated into the daughter nucleosome at random. Newly synthesized histone marks, e.g., acetylated lysine, are erased by histone deacetylases (HDACs). Methylated marks derived from parental histones that are next to newly incorporated histones are recognized by heterochromatin protein 1 (HP1), which forms a complex with histone methyltransferase (HMT). Subsequently, erased marks in the newly incorporated histones are quickly methylated by HMT. In this manner, histone modification patterns in a specific region of the genome are precisely copied. In addition, a semi-conservative model in which only dimers of H3–H4 tetramer are reused during nucleosome formation and an asymmetric model in which interactions between two newly synthesized DNA strands have been proposed for the regulation of histone modification copying (10,18,19).

Other than DNA methylation and histone modification, non-coding RNA, microRNA, and polycomb group (PcG) protein complex are epigenetic factors that modulate chromatin higher structure and influence the cellular phenotype (20,21). These varieties of macromolecular architectures may regulate and integrate epigenome inheritance.

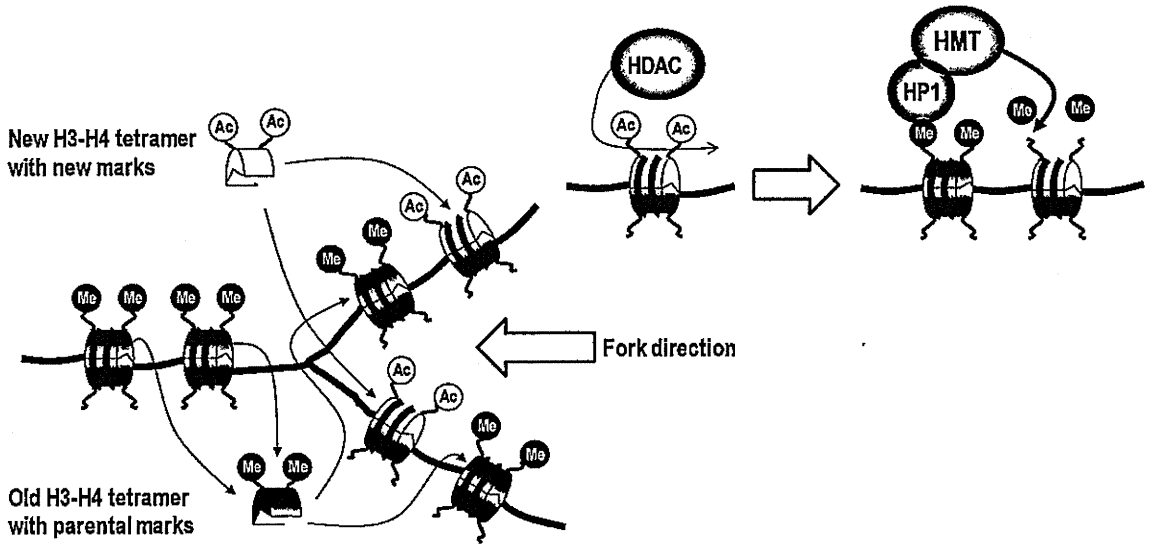

Fig. 1. A mechanistic representation of a hypothetical example of histone modification pattern inheritance. On newly synthesized DNA, parental histone H3–H4 tetramers are reused for the formation of the nucleosome of daughter chromatin. At the same time, newly synthesized histone H3–H4 tetramers are incorporated at random. The new histone marks (e.g., acetylated lysine) are erased by HDACs. Methylated marks derived from parental histones neighboring newly incorporated histones are recognized by HP1, which forms a complex with HMT. Erased marks in the newly incorporated histones are quickly methylated by HMT. In this manner, histone modification patterns in a specific region of the genome are precisely copied (19).

Human Disease and Epigenetics

In the retrospective cohort studies of David Barker and colleagues conducted in the United Kingdom, in which the country was divided into 212 local authority areas, a strong geographical relationship was observed between ischaemic heart disease mortality rates in 1968–78 and infant mortality in 1921–25 (1). Based on detailed epidemiological studies regarding the relationship between mother's birth weight and blood pressure, they concluded that babies who were small at birth or during infancy displayed increased rates of cardiovascular disease in adulthood (2). Moreover, they proposed the thrifty phenotype hypothesis, in which epidemiological associations between poor fetal and infant growth and the subsequent development of type 2 diabetes and metabolic syndrome are due to the effects of poor nutrition in early life, which produces permanent changes in glucose-insulin metabolism (22). The aforementioned theory is Barker's hypothesis, in which low maternal nutrition causes metabolic syndrome in offspring. Later termed the Developmental Origins of Health and Disease (DOHaD), the theory was expanded from Barker's hypothesis into the more general theory that health and disease susceptibility in the next generation depends on the environment surrounding the fertilized egg and fetuses in uterus, and throughout the neonatal life time (3,4,23).

Several attempts have recently been made to explain this phenomenon. The most reliable molecular mechanism underlying DOHaD is that epigenetic alternations that occur during the sensitive stage of fetus and newborn development persist into adulthood (5). In human studies, clear biochemical evidence has not yet been obtained; however, in laboratory animal experiments, the fetal environment, including physical and chemical factors altered epigenomic states such as DNA methylation and histone modification and persistent changes, influenced specific gene expression regulation (5). DOHaD has become more than a hypothesis and has been accepted by the clinical field. In the next section, animal studies related to DOHaD will be described.

Many carcinogeneses are known to be caused by aberrant DNA methylation, which is partially acquired in later stages of development. The hypermethylation of tumor suppressor genes such as *pRB* or *p16* is involved in retinoblastoma and epigenetic carcinogenesis (24,25). Clinical researchers are now considering epigenetic aberrations during carcinogenesis because DNA methyltransferase inhibitors are useful for cancer therapy (26–28). Thus, concern about chemically-induced epigenetic carcinogenesis in the next generation is increasing (6,8).

Animal Models Representing Epigenomic Changes Due to Perinatal Environmental Factors

Recently, a number of reports based on experimental animal models such as rats and mice demonstrated that *in utero* or neonatal nursing environmental stimuli altered DNA methylation and histone modification, which can persist into adulthood and potentially influence the phenotype (5,29). In most of these reports, clear and significant changes in the epigenome of specific target genes were detected. As described briefly below, in many of these reports, environmental chemicals including endocrine disruptors, which do not have mutagenic activities, were evaluated. Several leading papers are summarized in Table 1.

In rats, naturally occurring variations in maternal care influence the sensitivity of offspring to stress in adulthood. Meaney and colleagues at McGill University reported that the offspring of mothers that exhibited more licking and grooming of pups showed reduced plasma adrenocorticotropic hormone and corticosterone responses to acute stress, increased hippocampal glucocorticoid receptor (GR) mRNA expression, and enhanced glucocorticoid feedback sensitivity (30). Increased pup licking and grooming and arched-back nursing by rat mothers altered the offspring epigenome at a *Gr* gene promoter in the hippocampus, i.e., hypomethyaltion of CpG and increased histone acetylation and transcription factor (NGFI-A) binding (31). These studies revealed that maternal care determines offspring stress resistance in adulthood due to an altered level of epigenomic states in the brain.

Viable yellow (A^{vy}) mice are larger, obese, hyperinsulinemic, more susceptible to cancer, and shorter lived than their non-yellow siblings (32). They are epigenetic mosaics ranging from a yellow phenotype with maximum ectopic *Agouti* gene overexpression through a continuum of mottled *Agouti/yellow* phenotypes with partial *Agouti* overexpression to a pseudoagouti phenotype with minimal ectopic expression (32,33). This marked phenotypic change is significantly associated with the methylation level of CpG sites in an intracisternal A particle (IAP) retrotransposon upstream of the transcription start site of the *Agouti* gene. Feeding pregnant dams methyl-supplemented diets alters the epigenetic regulation of *Agouti* expression in their offspring, as indicated by increased *Agouti/black* mottling in the direction of the pseudoagouti phenotype (34). Maternal dietary genistein supplementation shifted the coat color of heterozygous viable yellow offspring toward pseudoagouti by hypermethylation of CpG sites in the retrotransposon of the *Agouti* gene (35). Furthermore, maternal exposure to bisphenol-A, an endocrine disruptor, shifted the coat color toward yellow by hypomethylation of retrotransposon CpG sites. Moreover, mater-

Table 1. Leading reports describing transgenerational effects of chemical exposures on epigenomic alternations in experimental animal models

Report	Animal	Chemicals	Dose	Period of exposure	Observed effects on phenotype	Detected changes in DNA methylation
Wu *et al.* (39)	ICR mouse	2,3,7,8-tetrachloro dibenzo-*p*-dioxin	10 nM *in vitro*	Fertilized egg with 1-2 cell or in the 8-cell stage	Reduced fetal body weight and reduced H19 mRNA expression	Hypermethyaltion of *H19/Igf2* genomic imprint region of DNA from the fetal body
Anway *et al.* (50) Crews *et al.* (52)	Sprague-Dawly rats	Vinclozolin Methoxychlor	100 mg/kg/day mother bw ip (Vinclozolin) 200 mg/kg/day mother bw ip (Methoxychlor)	Day 8 to day 15 of gestation	Germ cell apoptosis, decreased sperm count, decreased sexual preference for normal females in male offspring (F1-F4)	Hypomethylation of *Lplase* and cytokine-inducible SH2 protein genes in sperm DNA
Dolinoy *et al.* (35)	A^{vy} mouse	Genistein	250 mg/kg diet	2 weeks before mating through weaning	Coat-color change (a decease in yellow color and an increase pseudoagouti phenotype)	Hypermethylation of IAP insertion of the *Agouti* gene promoter region in skin DNA
Doliney *et al.* (36)	A^{vy} mouse	Bisphenol-A	50 mg/kg diet	2 weeks before mating through weaning	Coat-color change (an increase in yellow color and a decrease in the pseudoagouti phenotype)	Hypomethylation of IAP insertion of the *Agouti* gene promoter region in skin DNA
Onishchenko *et al.* (38)	C57BL/6kl mouse	Methylmercury	0.5 mg/kg/day via drinking water	Day 7 of gestation to day 7 of the postnatal period	Depression-like behavior and hippocampal BDNF mRNA suppression	Hypermethyaltion of hippocampal *Bdnf* promoter
Bromer *et al.* (37)	CD-1 mouse	Diethylstilbestrol	10 μg/kg/day mother bw ip	Day 9 to day 16 of gestation	Abnormalities in the reproductive tract and decreased homeobox A10 expression	Hypermethyaltion of uterus homeobox A10 gene intron

nal dietary supplementation with methyl donors such as folic acid or genistein negated the DNA hypomethylating effect of bisphenol-A (36).

Diethylstilbestrol (DES), a nonsteroidal estrogen, induces developmental anomalies in the female reproductive tract including vaginal cancer in humans perinatally exposed to DES. The expression of homeobox gene *Hoxa10*, which controls uterine organogenesis, is repressed in DES-exposed mouse offspring (37). In the mouse model, CpG methylation frequency in the *Hoxa10* intron was greater in DES-exposed offspring than control mice and was accompanied by increased expression of DNMT1 and DNMT3b.

Perinatal exposure to methylmercury causes persistent changes in learning and motivational behavior in C57BL/6 mice. Behavioral alterations are associated with a decrease in brain-derived neurotrophic factor (BDNF) mRNA in the hippocampal dentate gyrus. In this mouse experiment, methylmercury exposure caused the chromatin structure at the *Bdnf* promoter region to enter into a long-lasting repressive state. In particular, DNA hypermethylation, an increase in histone H3-K27 tri-methylation, and a decrease in H3 acetylation were observed at promoter IV (38).

2,3,7,8-Tetrachlorodibenzo-*p*-dioxin (TCDD) is the most toxic environmental pollutant. Short term exposure of preimplantation ICR mouse embryos to TCDD (10 nM) during the 1-cell stage to the blastocyst stage resulted in reduced fetal weight compared to unexposed preimplanted embryos. A decrease in the level of expression of imprinted genes *H19* and *Igf2* was observed, along with in an increase in the methylation frequency of the *H19/Igf2* imprint control region due to an increase in the paternal methylation status (39).

Perinatal exposure to a low dose of TCDD (environmental contamination levels) induces various types of developmental abnormalities in the offspring of laboratory animals (40,41). The cellular target molecule is an arylhydrocarbon receptor (AHR), which mediates every outcome of low dose TCDD toxicity (42). AHR can bind to polycyclic aromatic hydrocarbon mutagens such as benzo[*a*]pyrene (BaP) and 7,12-dimethylbenz[*a*]anthracene (DMBA) and can transactivate downstream target genes, including cytochrome P450 (CYP) family 1A1 and 1B1, which are phase I drug metabolizing enzymes (43). Using its monooxygenase activity, CYPs convert the mutagen into a reactive epoxide, which produces a covalent bond to the guanine residue in DNA and results in nucleotide mutation (44). In contrast, TCDD is a stable compound in the environment and living bodies; thus, TCDD cannot bind to DNA directly and induce mutations in nucleotide sequences. Female Sprague-Dawley rats exposed to TCDD in the fetal stage were more prone to DMBA-induced mammary tumors in adulthood than control rats

(45). Very low doses of 3,3′,4,4′,5-pentachlorobiphenyl (PCB126), which has a similar bioactivity to that of TCDD, had the same effect on DMBA-induced mammary tumor models when administered during pregnancy (46). Moreover, the induction state of *Cyp1a1* and *Cyp1b1* genes in the liver were enhanced after DMBA injection (47). The acceleration of *Cyp1* transcription resulted in higher carcinogenic susceptibility due to epigenetic alternations. In our laboratory, we demonstrated that C57BL/6J mice administered TCDD during the fetal stage showed a higher incidence of forestomach cancer due to BaP injection and enhanced induction of Cyp1a1 mRNA by TCDD re-administration in adulthood. Methyl-CpGs level of the *Cyp1a1* promoter region, which includes Ahr-binding xenobiotic response elements, is involved in TCDD induced transcription activity in LNCaP cells (48). The methylation frequency of the *Cyp1a1* promoter region in the liver DNA of mice exposed to TCDD was significantly lower than that of the control mice. Moreover, acetylation levels of histone H3 and H4 were significantly higher in TCDD-exposed mice (unpublished observations).

In laboratory studies conducted on animals, substantial evidence suggests that perinatal exposure to chemicals alters the epigenetic program of sensitive organs and persists into adulthood, affecting disease susceptibility. The mechanism of epigenomic status modulation, CpG hyper/hypomethylation, and maintenance of increased histone acetylation/methylation is still unclear; however, investigations are currently being conducted by many researchers.

Transgenerational Effects and Possible Lamarckian Inheritance

According to Barker's hypothesis, offspring phenotypes such as cardiovascular disease, risk of cancer, hypertension, and diabetes are thought to be inherited by the next generation (49). The epigenome alternations summarized in the present review can be inherited by the later generation via germ cell lines. Skinner and colleagues at Washington State University administered endocrine disruptors, fungicide vinclozolin and pesticide methoxychlor, to pregnant Sprague-Dawley rats to investigate spermatogenic defects and other toxic endpoints in male offspring (50). Transient exposure of vinclozolin, which does not display mutagenic activity, induced decreased spermatogenic capacity in adult phenotypes of the F_1 generation (sperm count and viability) and increased incidence of male infertility. These effects were transferred through the male germ line to nearly all of the males of subsequent generations, i.e., F_1 to F_4 (50,51). Moreover, male rats whose progenitors had been treated with vinclozolin showed lowered mate preference from control females (52). Using an arbitrary primer PCR and methylation sensitive restriction enzyme *Hpa*II, the authors demonstrated that the methylation pattern of lysophospholipase (*Lplase*) and cytokine-inducible SH2 protein genes was altered in the epididymal sperm DNA of F_2 and F_3 animals (50). Most recently, using a methylated DNA immunoprecipitation technique based on methyl-cytosine antibodies and a promoter tilling microarray (MeDIP-Chip) procedure, Skinner and coworkers identified 52 different regions in the sperm promoter epigenome with altered methylation patterns due to maternal exposure of vinclozolin (53). The series of studies conducted by Skinner's group suggest that a phenotype can be acquired by maternal exposure to environmental factors, leading to evolutional changes in animals. However, these studies are somewhat controversial because experiments focused on *Lplase* gene hypomethylation have not been reproduced using an identical protocol (54).

Compared to the offspring of males fed a control diet, the offspring of males fed a low-protein diet exhibited elevated hepatic expression of many genes involved in lipid and cholesterol biosynthesis and decreased levels of cholesterol esters (55). Epigenomic profiling of offspring livers via deep sequencing technology revealed numerous changes in CpG methylation due to alterations in the paternal diet, including reproducible changes in methylation over a likely enhancer for *Ppara*, a key lipid regulator. The results indicated that the parental diet can affect cholesterol and lipid metabolism in offspring, and a model system to study the environmental reprogramming of the heritable epigenome was defined. Acquired characteristics in the next generation may be inherited through the epigenome of paternal germlines. However, differences in sperm DNA methylation were not detected via deep sequencing (55). The epigenetic inheritance of RNA molecules has been described, and the expression of unusual *Kit* RNAs in the male germline (spermatozoon) of mice resulted in a phenotypic effect (on coat color) on the progeny of affected mice. In particular, two genetically identical mice differed phenotypically based on their parents' genotypes (56). These reports imply that untranslated RNAs can be potent epigenetic modulators for transgenerational effects on acquired characteristics rather than DNA methylation (57).

In the middle of the last century, Lysenko, a Russian plant biologist, emphasized his theory by conducting nutritional hybrid experiments and suggested that a white albino tomato could be transformed into a red tomato. Moreover, he suggested that autumn wheat could become spring wheat by applying low temperature treatments; however, little evidence was presented in these experiments. The aforementioned work was based on Lemarckian inheritance, i.e., the inheritance of an acquired phenotype. The theories of Lamarck and Lysenko have been neglected in the twentieth century.

However, the name of Lysenko, a very infamous one, is rising again in this century, due to the growth of epigenetics (58). Epigenetic transgenerational effects may alter germlines, and unknown factors other than DNA methylation or non-coding RNAs may be involved. The progress of research on acquired phenotypes will have a significant effect on perinatal medical aspects.

Acknowledgments: The author gratefully acknowledge Dr Kayoko Shimoi of the University of Shizuoka and Dr Tohru Shibuya for providing the opportunity to submit the manuscript to Genes and Environment.

References

1 Barker DJ, Osmond C. Infant mortality, childhood nutrition, and ischaemic heart disease in England and Wales. Lancet. 1986; 1: 1077–81.
2 Barker DJ, Shiell AW, Barker ME, Law CM. Growth *in utero* and blood pressure levels in the next generation. J Hypertens. 2000; 18: 843–6.
3 Sinclair KD, Lea RG, Rees WD, Young LE. The developmental origins of health and disease: current theories and epigenetic mechanisms. Soc Reprod Fertil Suppl. 2007; 64: 425–43.
4 Swanson JM, Entringer S, Buss C, Wadhwa PD. Developmental origins of health and disease: environmental exposures. Semin Reprod Med. 2009; 27: 391–402.
5 Rosenfeld CS. Animal models to study environmental epigenetics. Biol Reprod. 2010; 82: 473–88.
6 LeBaron MJ, Rasoulpour RJ, Klapacz J, Ellis-Hutchings RG, Hollnagel HM, Gollapudi BB. Epigenetics and chemical safety assessment. Mutat Res. 2010; 705: 83–95.
7 Bernal AJ, Jirtle RL. Epigenomic disruption: the effects of early developmental exposures. Birth Defects Res A Clin Mol Teratol. 2010; 88: 938–44.
8 Goodman JI, Augustine KA, Cunnningham ML, Dixon D, Dragan YP, Falls JG, Rasoulpour RJ, Sills RC, Storer RD, Wolf DC, Pettit SD. What do we need to know prior to thinking about incorporating an epigenetic evaluation into safety assessments? Toxicol Sci. 2010; 116: 375–81.
9 Ho DH, Burggren WW. Epigenetics and transgenerational transfer: a physiological perspective. J Exp Biol. 2010; 213: 3–16.
10 Corpet A, Almouzni G. Making copies of chromatin: the challenge of nucleosomal organization and epigenetic information. Trends Cell Biol. 2009; 19: 29–41.
11 Bostick M, Kim JK, Esteve PO, Clark A, Pradhan S, Jacobsen SE. UHRF1 plays a role in maintaining DNA methylation in mammalian cells. Science. 2007; 317: 1760–4.
12 Bestor T, Laudano A, Mattaliano R, Ingram V. Cloning and sequencing of a cDNA encoding DNA methyltransferase of mouse cells. The carboxyl-terminal domain of the mammalian enzymes is related to bacterial restriction methyltransferases. J Mol Biol. 1988; 203: 971–83.
13 Iida T, Suetake I, Tajima S, Morioka H, Ohta S, Obuse C, Tsurimoto T. PCNA clamp facilitates action of DNA cytosine methyltransferase 1 on hemimethylated DNA. Genes Cells. 2002; 7: 997–1007.
14 Comb M, Goodman HM. CpG methylation inhibits proenkephalin gene expression and binding of the transcription factor AP-2. Nucleic Acids Res. 1990; 18: 3975–82.
15 Rideout WM 3rd, Eversole-Cire P, Spruck CH 3rd, Hustad CM, Coetzee GA, Gonzales FA, Jones PA. Progressive increases in the methylation status and heterochromatinization of the myoD CpG island during oncogenic transformation. Mol Cell Biol. 1994; 14: 6143–52.
16 Reik W, Dean W, Walter J. Epigenetic reprogramming in mammalian development. Science. 2001; 293: 1089–93.
17 Shilatifard A. Chromatin modifications by methylation and ubiquitination: implications in the regulation of gene expression. Annu Rev Biochem. 2006; 75: 243–69.
18 Turner BM. Cellular memory and the histone code. Cell. 2002; 111: 285–91.
19 Probst AV, Dunleavy E, Almouzni G. Epigenetic inheritance during the cell cycle. Nat Rev Mol Cell Biol. 2009; 10: 192–206.
20 Djupedal I, Ekwall K. Epigenetics: heterochromatin meets RNAi. Cell Res. 2009; 19: 282–95.
21 Francis NJ. Mechanisms of epigenetic inheritance: copying of polycomb repressed chromatin. Cell Cycle. 2009; 8: 3513–8.
22 Hales CN, Barker DJ. The thrifty phenotype hypothesis. Br Med Bull. 2001; 60: 5–20.
23 Wadhwa PD, Buss C, Entringer S, Swanson JM. Developmental origins of health and disease: brief history of the approach and current focus on epigenetic mechanisms. Semin Reprod Med. 2009; 27: 358–68.
24 Ohtani-Fujita N, Dryja TP, Rapaport JM, Fujita T, Matsumura S, Ozasa K, Watanabe Y, Hayashi K, Maeda K, Kinoshita S, Matsumura T, Ohnishi Y, Hotta Y, Takahashi R, Kato MV, Ishizaki K, Sasaki MS, Horsthemke B, Minoda K, Sakai T. Hypermethylation in the retinoblastoma gene is associated with unilateral, sporadic retinoblastoma. Cancer Genet Cytogenet. 1997; 98: 43–9.
25 Esteller M. CpG island hypermethylation and tumor suppressor genes: a booming present, a brighter future. Oncogene. 2002; 21: 5427–40.
26 McCabe MT, Low JA, Daignault S, Imperiale MJ, Wojno KJ, Day ML. Inhibition of DNA methyltransferase activity prevents tumorigenesis in a mouse model of prostate cancer. Cancer Res. 2006; 66: 385–92.
27 Ushijima T. Detection and interpretation of altered methylation patterns in cancer cells. Nat Rev Cancer. 2005; 5: 223–31.
28 Ushijima T, Asada K. Aberrant DNA methylation in contrast with mutations. Cancer Sci. 2010; 101: 300–5.
29 McMullen S, Mostyn A. Animal models for the study of the developmental origins of health and disease. Proc Nutr Soc. 2009; 68: 306–20.
30 Liu D, Diorio J, Tannenbaum B, Caldji C, Francis D, Freedman A, Sharma S, Pearson D, Plotsky PM, Meaney MJ. Maternal care, hippocampal glucocorticoid receptors, and hypothalamic-pituitary-adrenal responses to

stress. Science. 1997; 277: 1659–62.
31 Weaver IC, Cervoni N, Champagne FA, D'Alessio AC, Sharma S, Seckl JR, Dymov S, Szyf M, Meaney MJ. Epigenetic programming by maternal behavior. Nat Neurosci. 2004; 7: 847–54.
32 Yen TT, Gill AM, Frigeri LG, Barsh GS, Wolff GL. Obesity, diabetes, and neoplasia in yellow A(vy)/-mice: ectopic expression of the agouti gene. Faseb J. 1994; 8: 479–88.
33 Wolff GL, Kodell RL, Moore SR, Cooney CA. Maternal epigenetics and methyl supplements affect agouti gene expression in Avy/a mice. Faseb J. 1998; 12: 949–57.
34 Waterland RA, Jirtle RL. Transposable elements: targets for early nutritional effects on epigenetic gene regulation. Mol Cell Biol. 2003; 23: 5293–300.
35 Dolinoy DC, Weidman JR, Waterland RA, Jirtle RL. Maternal genistein alters coat color and protects Avy mouse offspring from obesity by modifying the fetal epigenome. Environ Health Perspect. 2006; 114: 567–72.
36 Dolinoy DC, Huang D, Jirtle RL. Maternal nutrient supplementation counteracts bisphenol A-induced DNA hypomethylation in early development. Proc Natl Acad Sci USA. 2007; 104: 13056–61.
37 Bromer JG, Wu J, Zhou Y, Taylor HS. Hypermethylation of homeobox A10 by *in utero* diethylstilbestrol exposure: an epigenetic mechanism for altered developmental programming. Endocrinology. 2009; 150: 3376–82.
38 Onishchenko N, Karpova N, Sabri F, Castren E, Ceccatelli S. Long-lasting depression-like behavior and epigenetic changes of BDNF gene expression induced by perinatal exposure to methylmercury. J Neurochem. 2008; 106: 1378–87.
39 Wu Q, Ohsako S, Ishimura R, Suzuki JS, Tohyama C. Exposure of mouse preimplantation embryos to 2,3,7,8-tetrachlorodibenzo-*p*-dioxin (TCDD) alters the methylation status of imprinted genes *H19* and *Igf2*. Biol Reprod. 2004; 70: 1790–7.
40 Mably TA, Moore RW, Goy RW, Peterson RE. *In utero* and lactational exposure of male rats to 2,3,7,8-tetrachlorodibenzo-p-dioxin. 2. Effects on sexual behavior and the regulation of luteinizing hormone secretion in adulthood. Toxicol Appl Pharmacol. 1992; 114: 108–17.
41 Ohsako S, Miyabara Y, Sakaue M, Ishimura R, Kakeyama M, Izumi H, Yonemoto J, Tohyama C. Developmental stage-specific effects of perinatal 2,3,7,8-tetrachlorodibenzo-*p*-dioxin exposure on reproductive organs of male rat offspring. Toxicol Sci. 2002; 66: 283–92.
42 Ohsako S, Fukuzawa N, Ishimura R, Kawakami T, Wu Q, Nagano R, Zaha H, Sone H, Yonemoto J, Tohyama C. Comparative contribution of the aryl hydrocarbon receptor gene to perinatal stage development and dioxin-induced toxicity between the urogenital complex and testis in the mouse. Biol Reprod. 2010; 82: 636–43.
43 Whitlock JP Jr. Induction of cytochrome P4501A1. Annu Rev Pharmacol Toxicol. 1999; 39: 103–25.
44 Sims P, Grover PL, Swaisland A, Pal K, Hewer A. Metabolic activation of benzo[*a*]pyrene proceeds by a diol-epoxide. Nature. 1974; 252: 326–8.
45 Brown NM, Manzolillo PA, Zhang JX, Wang J, Lamartiniere CA. Prenatal TCDD and predisposition to mammary cancer in the rat. Carcinogenesis. 1998; 19: 1623–9.
46 Muto T, Wakui S, Imano N, Nakaaki K, Takahashi H, Hano H, Furusato M, Masaoka T. Mammary gland differentiation in female rats after prenatal exposure to 3,3′,4,4′,5-pentachlorobiphenyl. Toxicology. 2002; 177: 197–205.
47 Wakui S, Yokoo K, Takahashi H, Muto T, Suzuki Y, Kanai Y, Hano H, Furusato M, Endou H. Prenatal 3,3′,4,4′,5-pentachlorobiphenyl exposure modulates induction of rat hepatic CYP 1A1, 1B1, and AhR by 7,12-dimethylbenz[*a*]anthracene. Toxicol Appl Pharmacol. 2006; 210: 200–11.
48 Okino ST, Pookot D, Li LC, Zhao H, Urakami S, Shiina H, Igawa M, Dahiya R. Epigenetic inactivation of the dioxin-responsive cytochrome P4501A1 gene in human prostate cancer. Cancer Res. 2006; 66: 7420–8.
49 Jirtle RL, Skinner MK. Environmental epigenomics and disease susceptibility. Nat Rev Genet. 2007; 8: 253–62.
50 Anway MD, Cupp AS, Uzumcu M, Skinner MK. Epigenetic transgenerational actions of endocrine disruptors and male fertility. Science. 2005; 308: 1466–9.
51 Skinner MK, Anway MD. Seminiferous cord formation and germ-cell programming: epigenetic transgenerational actions of endocrine disruptors. Ann N Y Acad Sci. 2005; 1061: 18–32.
52 Crews D, Gore AC, Hsu TS, Dangleben NL, Spinetta M, Schallert T, Anway MD, Skinner MK. Transgenerational epigenetic imprints on mate preference. Proc Natl Acad Sci USA. 2007; 104: 5942–6.
53 Guerrero-Bosagna C, Settles M, Lucker B, Skinner MK. Epigenetic transgenerational actions of vinclozolin on promoter regions of the sperm epigenome. PLoS One. 2010; 5: e13100.
54 Inawaka K, Kawabe M, Takahashi S, Doi Y, Tomigahara Y, Tarui H, Abe J, Kawamura S, Shirai T. Maternal exposure to anti-androgenic compounds, vinclozolin, flutamide and procymidone, has no effects on spermatogenesis and DNA methylation in male rats of subsequent generations. Toxicol Appl Pharmacol. 2009; 237: 178–87.
55 Carone BR, Fauquier L, Habib N, Shea JM, Hart CE, Li R, Bock C, Li C, Gu H, Zamore PD, Meissner A, Weng Z, Hofmann HA, Friedman N, Rando OJ. Paternally induced transgenerational environmental reprogramming of metabolic gene expression in mammals. Cell. 2010; 143: 1084–96.
56 Rassoulzadegan M, Grandjean V, Gounon P, Vincent S, Gillot I, Cuzin F. RNA-mediated non-mendelian inheritance of an epigenetic change in the mouse. Nature. 2006; 441: 469–74.
57 Rando OJ, Verstrepen KJ. Timescales of genetic and epigenetic inheritance. Cell. 2007; 128: 655–68.
58 Maderspacher F. Lysenko rising. Curr Biol. 2010; 20: R835–7.

ANATOMIA HISTOLOGIA EMBRYOLOGIA
JOURNAL OF VETERINARY MEDICINE

Anatomia Histologia Embryologia

ORIGINAL ARTICLE

Di(*n*-butyl) Phthalate Induces Vimentin Filaments Disruption in Rat Sertoli Cells: A Possible Relation with Spermatogenic Cell Apoptosis

M. S. Alam[1], S. Ohsako[2], T. W. Tay[1], N. Tsunekawa[1], Y. Kanai[1] and M. Kurohmaru[1]*

Addresses of authors: [1] Department of Veterinary Anatomy, Graduate School of Agricultural and Life Sciences, The University of Tokyo, 1-1-1 Yayoi, Bunkyo-ku, Tokyo 113-8657, Japan;
[2] Laboratory of Environmental Health Sciences, Center for Disease Biology and Integrative Medicine, Graduate School and Faculty of Medicine, The University of Tokyo, 7-3-1 Hongo, Bunkyo-ku, Tokyo 113-0033

***Correspondence:**
Tel.: +81 (3) 5841 5384;
fax: +81 (3) 5841 8181,
e-mail: amkuroh@mail.ecc.u-tokyo.ac.jp

With 3 figures

Received January 2010; accepted for publication January 2010

doi: 10.1111/j.1439-0264.2010.00993.x

Summary

Phthalate esters have been extensively used as a plasticizer of synthetic polymers. Previous studies have revealed that some phthalate esters including di(*n*-butyl) phthalate (DBP) induce spermatogenic cell apoptosis, although its mechanism is not yet clear. The present study describes that disruption of Sertoli cell vimentin filaments by DBP administration may relate to spermatogenic cell apoptosis. The present histopathological study revealed that a single oral administration of 500 mg/kg DBP caused progressive detachment and displacement of spermatogenic cells away from the seminiferous epithelium and sloughing of them into the lumen. Degenerative spermatogenic cells characterized by chromatin condensation were frequently observed in DBP-treated rats. Ultrastructurally, the degenerative spermatogenic cells were separated from their neighbours, and a collapse of Sertoli cell vimentin filaments was recognized in DBP-treated rats. Sertoli cell cultures showed the increased number and size of vacuoles in their cytoplasm. In agreement with the *in vivo* experiment, vimentin filaments clearly showed a gradual collapse in DBP-exposed Sertoli cells *in vitro*. These *in vivo* and *in vitro* experiments indicate that DBP-induced collapse of Sertoli cell vimentin filaments may lead to detachment of spermatogenic cells, and then detached cells may undergo apoptosis because of loss of the support and nurture provided by Sertoli cells.

Introduction

Di(*n*-butyl) phthalate (DBP), one of heavily used phthalate esters, is widely used as a plasticizer in cosmetics, printing inks and pharmaceutical coating. Phthalate esters including DBP have been shown to induce testicular atrophy. To date, several mechanisms have been proposed to explain the induction of testicular atrophy by phthalate esters. For example, the depletion of zinc in testes was induced by monobutyl phthalate (MBP) and mono(2-ethylhexyl) phthalate (MEHP), metabolites of DBP and di(2-ethylhexyl) phthalate (DEHP), respectively (Oishi and Hiraga, 1980). Membrane alteration of Sertoli cells induced by MEHP would lead to separation of spermatogenic cells from underlying Sertoli cells (Gray and Beamand, 1984; Richburg and Boekelheide, 1996; Tay et al., 2007). Upregulation of Fas and Fas ligand gene induced by MEHP activated spermatogenic cell apoptosis (Lee et al., 1997; 1999; Richburg et al., 1999). However, the primary cellular target or mechanism of DBP-induced spermatogenic cell apoptosis is not yet clear.

The interaction between Sertoli and spermatogenic cells is crucially important for successful spermatogenesis, because Sertoli cells form sites of attachment to spermatogenic cells. These Sertoli cells possess a highly organized and quite active cytoskeleton. The cytoskeleton consists of three major components, namely, microfilaments (actin), intermediate filaments and microtubules

(tubulin). In Sertoli cells, intermediate filaments are of vimentin type, with a molecular weight of 55–58 kDa (Franke et al., 1979). Vimentin filaments, formed by polymerization of 57 kDa vimentin monomers, surround the nucleus, give it the characteristic 'halo' appearance (Show et al., 2003), radiate outward to the cell periphery, and terminate near points of contact between Sertoli cell and adjacent cells. Vimentin filaments mediate the tight junction between neighbouring Sertoli cells, as well as the desmosome-like junction located between Sertoli cells and spermatogenic cells and the ectoplasmic specialization between Sertoli cells and more advanced spermatogenic cells. It has been suggested that vimentin filaments play a role in positioning the Sertoli cell nucleus and anchoring spermatogenic cells to the seminiferous epithelium (Amlani and Vogl, 1988), or act as a mediator of cell signal transduction between the plasma membrane and nucleus. Thus, they are essentially important for spermatogenesis (Aumuller et al., 1988, 1992). On the contrary, the collapse of vimentin filaments after xenobiotic treatment correlated with the loss of structural integrity of the seminiferous epithelium, along with spermatogenic cell apoptosis (Johnson et al., 1991; Richburg and Boekelheide, 1996; Dalgaard et al., 2001).

Phthalate esters disrupt Sertoli-spermatogenic cell contacts in post-natal Sertoli-spermatogenic cell co-cultures several hours after exposure (Gray and Beamand, 1984) and alter signalling modulated by follicle-stimulating hormone in cultured Sertoli cells (Heindel and Chapin, 1989; Grasso et al., 1993). In prepubertal rats, an acute exposure to MEHP resulted in collapsed Sertoli cell vimentin filaments and spermatogenic cell sloughing (Richburg and Boekelheide, 1996). Our previous study using an *in vitro* model, primary Sertoli cell culture, has also reported that MEHP disrupts vimentin filaments in mice Sertoli cells several hours after administration (Tay et al., 2007). Unfortunately, the mechanism underlying the cytotoxic effects of DBP on spermatogenic cell apoptosis, as well as the effects on Sertoli cell vimentin filaments, is not completely understood. Thus, the aim of this study was to examine a specific and early DBP-induced collapse of Sertoli cell vimentin filaments *in vivo* and *in vitro* and correlation between collapse of vimentin filaments and previously reported time course rates of spermatogenic cell apoptosis induced by a single DBP administration (Alam et al., 2010).

Materials and Methods

Animals and treatments

Male Sprague-Dawley (SD) rats (3-week-old) were purchased from Charles River Laboratories Japan (Tokyo, Japan). The rats were housed three to five per one plastic cage, maintained on a 12-h light/dark cycle at a constant temperature (22 ± 1°C) and humidity (45–70%), and provided water and rodent pellets (Oriental Yeast, Tokyo, Japan) *ad libitum*. Animals were maintained and handled humanely in accordance with the guideline of the animal experiments of the Institutional Animal Care and Use Committee (IACUC) of the University of Tokyo, Tokyo, Japan.

Three-week-old male rats ($n = 8$) were given a single oral administration of 500 mg/kg DBP in vehicle at a volume equal to 4 ml/kg. The vehicle was a mixture of 5% ethanol and 95% corn oil. Control animals received the same volume of vehicle. Rats were then killed under diethyl ether anaesthesia at 6 and 24 h after administration, and their testes were collected and subjected to histopathology.

The chosen dose of DBP was based on our earlier report in which a single administration of 500 mg/kg was sufficient for significantly increased number of spermatogenic cell apoptosis (Alam et al., 2010).

Sertoli cell culture and DBP treatment

Mixed cultures of Sertoli and spermatogenic cells were prepared from 3-week-old SD rats as described earlier (Worrell et al., 1989; Tay et al., 2007) with adaptations, and were maintained at 32°C in 25 cm^2 tissue culture flasks. In brief, testes were excised, decapsulated, cut into smaller pieces, and treated with 0.1% collagenase (Sigma, St. Louis, MO, USA). Single cells were obtained by gravity sedimentation and usage of 50% trypsin-EDTA (Gibco, Michele Serro, NY, USA). Cells were finally suspended at a concentration of 1×10^8 cell/ml and maintained for 24 h in Dulbecco's modified Eagle medium (Sigma) supplemented with 100 U/ml penicillin, 100 μg/ml streptomycin (Gibco), and 10% fetal bovine serum (Sigma). Thereafter, cells were maintained in serum-free medium, which was changed every 24 h. At 72 h, spermatogenic cells were removed by treatment with hypotonic Tris buffer (20 mM Tris–HCL, pH 7.4) for 5 min as described by Galdieri et al. (1981). The Sertoli cell-enriched cultures obtained were then maintained in serum-free medium for 24 h before being reseeded onto chamber slides. The samples were cultured for further 5 days. Subsequently, they were exposed to 0, 0.1, 1, and 100 nmol/ml DBP for 6 and 24 h. Some slides were stained with 1% toluidine blue for light microscopic observations, whereas the rest were used for vimentin immunohistochemical analysis.

Light microscopy

For histopathological observations (haematoxylin and eosin or immunohistochemical staining), under diethyl

ether anesthesia, rats were perfused with 10% neutrally buffered formalin for 30 min. Following perfusion, the testes were excised and immersed in the same fixative for 48 h. Then, the samples were washed in 0.1 M phosphate buffer solution for 3 h, dehydrated through a graded series of ethanol, cleared in xylene, and embedded in paraffin. The paraffin blocks were cut at 4 μm in thickness. The sections were then stained with Meyer's haematoxylin and eosin and/or periodic acid-Schiff (PAS)-haematoxylin. They were observed by light microscopy.

Transmission electron microscopy

For transmission electron microscopy, under diethyl ether anaesthesia, rats were perfused with 5% glutaraldehyde in 0.1 M phosphate buffer. Then, the testes were excised, immersed in the same fixative at 4°C for 3 h and post-fixed in 1% osmium tetroxide (OsO_4) at 4°C for 2 h. The samples were then dehydrated in a graded series of ethanol, infiltrated in propylene oxide, and embedded in Araldite M. Semi-thin sections were cut at about 1 μm in thickness, stained with 1% toluidine blue, and observed by light microscopy. Ultrathin sections were cut, and stained with uranyl acetate and lead citrate. In the DBP-treated rats, unique lesions were encountered at the light microscopic level at 24 h. Corresponding tissue sections from these animals, along with appropriate control sections, were examined using a JEM-1010 transmission electron microscope at 80 kV (JEOL, Ltd, Tokyo, Japan). Evaluation was limited to characterization of subtle lesions and abnormal cells, because quantitative analysis is impractical with transmission electron microscopy.

Immunohistochemistry

For vimentin immunohistochemistry on primary Sertoli cell cultures, a monoclonal anti-vimentin antibody (mouse immunoglobulin M [IgM] isotype, clone LN-6; Sigma) at a dilution 1:200 was used for staining vimentin in Sertoli cells. Slides were fixed in 10% neutrally buffered formalin for 20 min, rinsed in PBS, blocked with a TNB (0.1 M Tris–HSC, 0.15 M MaCl, 0.5% blocking reagent, pH 7.5) blocking buffer, supplied in tyramide signal amplification (TSA) Biotin System Kit (Perkin Elmer Life Sciences, Boston, MA, USA), and incubated at 4°C overnight with primary antibody. Thereafter, the sections were incubated with biotinylated goat anti-mouse IgG secondary antibody for 1–2 h at room temperature, followed by the ABC kit (Funakoshi, Tokyo, Japan). Immunoreaction was visualized with 0.05% diaminobenzidine tetrahydrochloride (DAB) (Wako, Tokyo, Japan) with H_2O_2 in PBS. The sections were lightly counterstained with haematoxylin. For a negative control, the incubation step with the primary antibody was omitted.

For another immunohistochemistry, the sections were deparaffinized, rinsed in PBS, rehydrated, and latter heated in 0.01 M citrate buffer (pH 6.0) for 10 min in a microwave to facilitate antigen retrieval. They were treated with 3% H_2O_2 for 30 min to eliminate endogenous peroxidase, blocked with a TNB blocking buffer, and incubated at 4°C overnight with primary antibody. A monoclonal antibody to vimentin was used at a dilution of 1:200, mouse monoclonal anti-α tubulin (Clone DM 1A, Sigma) was 1:200 and mouse monoclonal anti-actin antibody (Clone 1A4, Sigma) was 1:5000 dilution. Thereafter, protocols were similar as described above.

Results

Histopathology

Histopathology was evaluated using cross-sections of seminiferous tubules by light (haematoxylin–eosin or toluidine blue staining) and transmission electron microscopies. In haematoxylin and eosin stained sections, detachment of spermatogenic cells away from the basement membrane and sloughing of them into the lumen were observed in the DBP-treated group, compared with the control (Fig. 1a–c). In semi-thin sections stained with toluidine blue (Fig. 1d–f), degenerative spermatogenic cells were easily detected by their condensed nuclear chromatin, one of the hallmarks of apoptotic cell death. Degenerative spermatogenic cells were frequently observed in the DBP-treated group, compared with the control (Fig. 1d–f). A maximum number of degenerative spermatogenic cells were detected at 6 h after treatment (Fig. 1e). By careful observations, some nuclear chromatin condensed cells surrounded by an empty space were recognizable. They might fall away from their neighbours. In transmission electron microscopic observations, it was apparently distinguishable that the degenerative spermatogenic cells detached from their neighbours were surrounded by an empty space at 6 h after DBP treatment, whereas normal spermatogenic cells had a close contact with their neighbours in the control (Fig. 1g, h). These degenerative spermatogenic cells appeared to be apoptotic in nature based on break in DNA when being visualized by *in situ* terminal deoxynucleotidyl transferase-mediated digoxigenin-dUTP nick end-labeling (TUNEL) method (data not shown).

Vimentin staining

Vimentin filaments were visualized by immunohistochemistry (Fig. 2a–c). In Sertoli cells of the control, vimentin filaments could be seen as projections extending from the

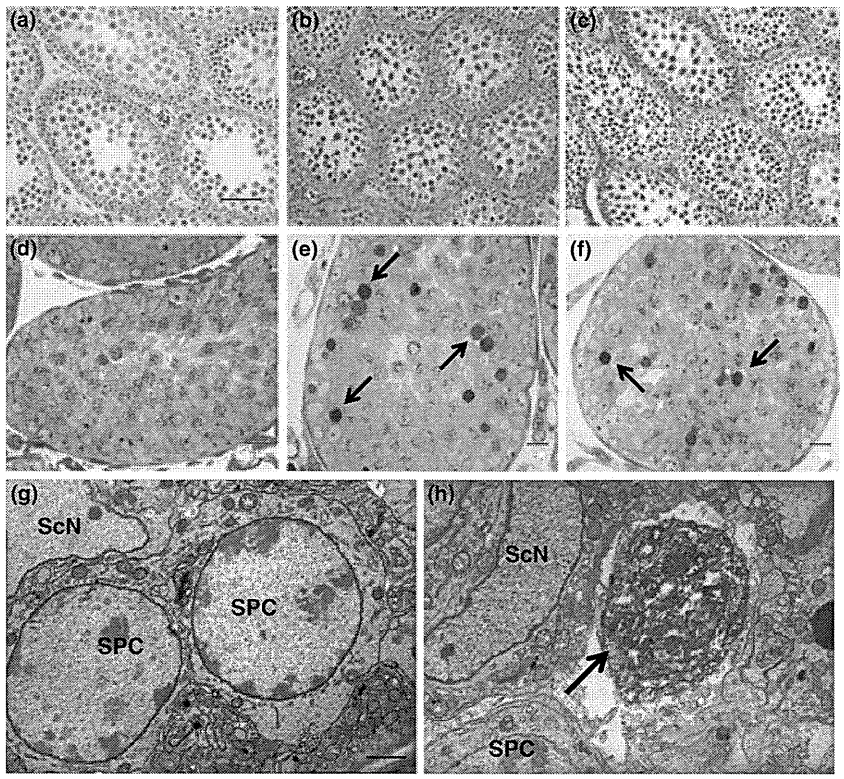

Fig. 1. Histological changes in testes after a single administration of 500 mg DBP/kg are shown. Haematoxylin and eosin staining sections (a–c), semi-thin sections stained with toluidine blue (d–f) and transmission electron micrographs (g–h). Control (a, d and g), at 6 h (b, e and h), and at 24 h (c and f) after treatment. Arrows indicate degenerative spermatogenic cells isolated by an empty space from their neighbours. ScN, Sertoli cell nucleus; SPC, spermatocyte. Scale bar, a–c = 50 μm, d–f = 30 μm, and g, h = 1 μm.

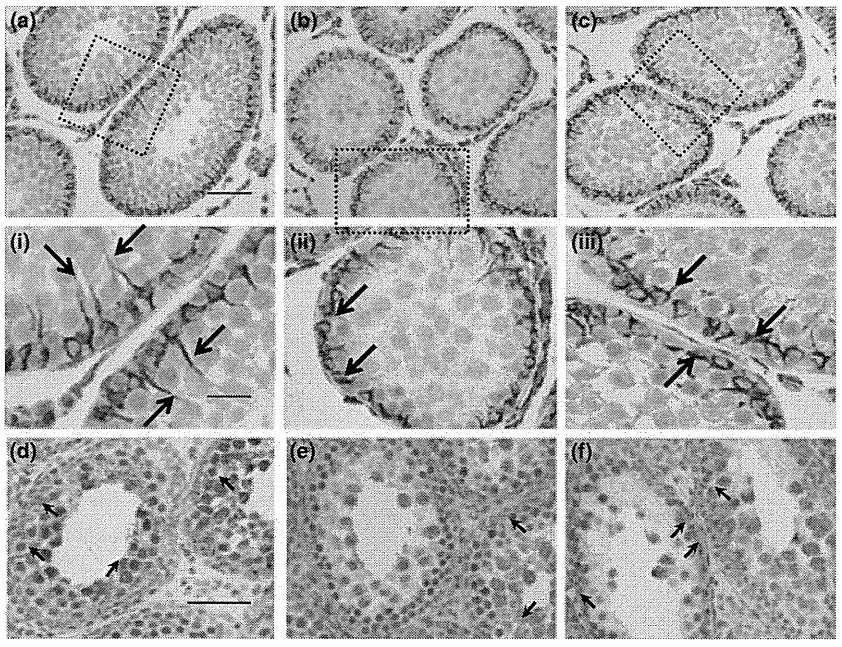

Fig. 2. Di(*n*-butyl) phthalate-induced cytoskeletal disruption in Sertoli cells is shown. Vimentin staining (a–c, i–iii) and actin staining (d–f). Control (a, i, d), at 6 h (b, ii, e), and at 24 h (c, iii, f) after treatment. Rectangles in a, b, and c are shown in i, ii, and iii at higher magnification, respectively. Note that in the control (a, i), vimentin filaments can be seen as projections extending from the perinuclear regions of Sertoli cell toward the lumen (arrows). Abundant apical extensions of vimentin filaments show collapsed and densely concentrated around the Sertoli cell nucleus (arrows) at 6 h (b, ii) and at 24 h (c, iii) after treatment. Actin (arrows) staining intensity is low in treated groups (e, f), compared with the control (d). Detachment and displacement of spermatogenic cells can also be seen in treated groups. Scale bar, a–c = 50 μm, i–iii, and d–f = 20 μm.

basal region towards the lumen (Fig. 2a, i). At 6 h after DBP administration, vimentin filaments showed shorter projections and concentrated near the basal region, while spermatogenic cells were detached away from the basement membrane and sloughed into the lumen (Fig. 2b, ii). At 24 h after treatment, a dramatic loss of vimentin filaments in apical extensions (Fig. 2c, iii) was detected, indicating the collapse of vimentin filaments in the DBP-treated rats.

To determine whether the effects of DBP were specific for Sertoli cell vimentin filaments, the staining pattern of α-tubulin was examined. The α-tubulin staining pattern was characterized by the long-defined tracts extending along the axis of the Sertoli cell. No difference was observed in distribution between the DBP-treated and control rats (data not shown). This finding demonstrated that DBP did not disrupt the Sertoli cell microtubule network. Actin staining in cross-sections of the control showed very strong in the basal region of Sertoli cells, probably corresponding to tight junctions and peripheral regions of spermatocytes (Fig. 2d), whereas the staining was weak in intensity in the DBP treated rats testes (Fig. 2e, f).

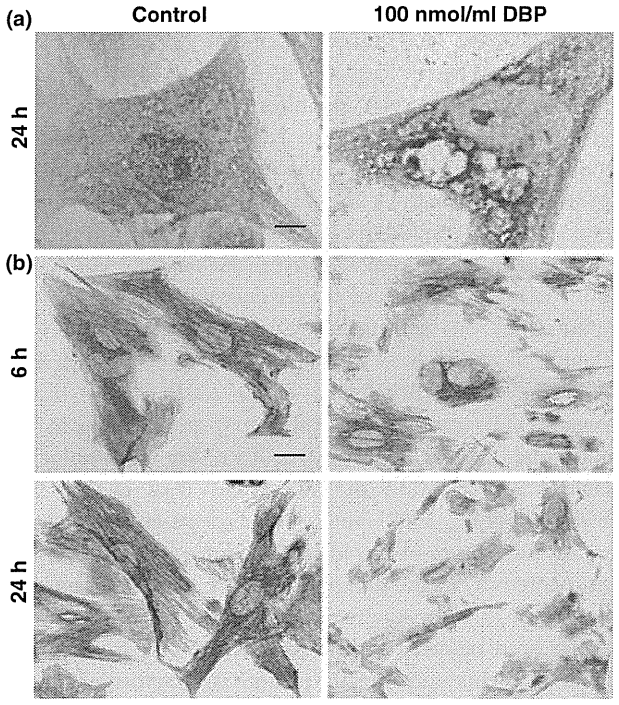

Fig. 3. Toluidine blue and vimentin staining in cultured Sertoli cells. At 24 h, 100 nmol/ml DBP-treated Sertoli cell shows severe vacuolation with multiple vacuoles, compared to vehicle-treated Sertoli cell (a). Vimentin filaments show severely collapsed and densely concentrated around the nucleus in 100 nmol/ml DBP-treated Sertoli cells at 6 and 24 h, compared to strong staining in the controls (b). Scale bar, a = 10 μm, b = 30 μm.

Primary Sertoli cell culture

Sertoli cells in culture treated with DBP and later stained with toluidine blue, showed the presence of vacuoles in the cytoplasm. The vacuoles were increased in number and size in time- and dose-dependant manners (data not shown). The maximum size and number of vacuoles were seen at highest dose (100 nmol/ml) for 24 h, compared with the control (Fig. 3a).

In order to clarify the vimentin expression in isolated Sertoli cells, we conducted anti-vimentin immunohistochemical staining in primary Sertoli cell cultures treated with DBP for 6 and 24 h. In the Sertoli cells control, vimentin filaments surrounded the Sertoli cell nucleus and radiated out from the nucleus to the cell periphery (Fig. 3b). Exposure to DBP caused a gradual collapse of vimentin filaments, and Sertoli cell conjunctions were detached. Thus, vimentin filaments were distributed only around the Sertoli cell nucleus in the treated groups, and gradually notable with increased concentrations of DBP. Vimentin expression was decreased with increased exposure time in 0.1 and 1 nmol/ml DBP treated groups (data not shown). Severe collapse of vimentin filaments was observed at 6 and 24 h in 100 nmol/ml treated groups, compared with the strong reaction noted in the control (Fig. 3b). Thus, *in vivo* and *in vitro* data clearly demonstrated that DBP exposure collapsed vimentin filaments in Sertoli cells.

Discussion

In earlier studies, rapid disruption of Sertoli cell-spermatogenic cell physical interactions, ultimately leading to detachment and sloughing of spermatogenic cells from the seminiferous epithelium, was observed after several Sertoli cell toxicants, including phthalate esters, administration (Creasy et al., 1987; Richburg and Boekelheide, 1996). The underlying mechanism for the detachment of spermatogenic cells away from the seminiferous epithelium induced by DBP has not yet been clarified. However, many researchers commonly believe that the Sertoli cell is the primary target of phthalate esters based upon Sertoli cell specific biochemical and morphological alterations after treatment (Creasy et al., 1983; Dostal et al., 1987; Lloyd and Foster, 1988; Boekelheide, 1993; Richburg and Boekelheide, 1996; Boekelheide et al., 2005). On this point, no data are available on DBP. Spermatogenic cell loss in the seminiferous epithelium was found to result from Sertoli cell dysfunction (Foster et al., 1982; Gray and Beamand, 1984). The Sertoli cell is responsible for orchestrating the differentiation of spermatogenic cells as well as providing nutritional and physiological supports (Aumuller et al., 1988, 1992).

In order to characterize the effects of DBP on Sertoli cells, we carried out two experiments: (1) *in vivo* experiment; a single administration of DBP to prepubertal rats to examine the early and specific effects of DBP on Sertoli cells-spermatogenic cells contact, (2) *In vitro* experiment; primary Sertoli cell cultures treated with DBP to examine the direct effect of DBP on morphology and collapse of vimentin filaments in isolated Sertoli cells. In *in vivo* observations, DBP-induced collapse of Sertoli cell vimentin filaments appears to be a reflection of detachment and displacement of spermatogenic cells away from basement membrane and sloughing of them into the lumen.

In cultured Sertoli cells stained with toluidine blue in the present study showed the presence of different-sized vacuoles. Higher concentration and longest exposure period of DBP revealed more dramatic morphological effects on Sertoli cells. It has been suggested that vacuolation in Sertoli cells is the earliest morphological sign of testicular injury, and the cardinal response is seen with many Sertoli cell toxicants (Creasy et al., 1987). In accordance with *in vivo* experiment, in *in vitro* experiment, we have also confirmed that the Sertoli cell cytoskeleton responds to DBP by exhibiting a marked collapse in vimentin filaments distribution in cultured Sertoli cells. Exposure to DBP collapses vimentin filaments, and then spermatogenic cell may detach from Sertoli cells in a dose-dependent manner. In the earlier reports, the collapse of Sertoli intermediate filaments has been observed in cryptorchid testes of immature rats *in vivo* (Wang et al., 2002; Kopecky et al., 2005); in such testes, immunohistochemical staining of vimentin filaments revealed loss of their extension and collapse at their perinuclear localization, coinciding with massive spermatogenic cell apoptosis. In addition, the break down of Sertoli cell intermediate filaments has also been reported in MEHP (Lloyd and Foster, 1988; Richburg and Boekelheide, 1996; Tay et al., 2007) or colchicine (Allard et al., 1993) treatment, resulting in loss of structural integrity of the seminiferous epithelium followed by spermatogenic cell apoptosis and sloughing. Similarly, alteration of Sertoli cell vimentin filaments distribution has been shown in 2,5-hexanedione (Hall et al., 1991) or fungicide benomyl (Hess and Nakai, 2000) administration and hormonal withdrawal (Show et al., 2003). Thus, the collapse of Sertoli cell vimentin filaments leads to detachment of spermatogenic cells from Sertoli cells, and that is the first step towards cell death. Since these vimentin-detached spermatogenic cells lost the support and nurture provided by Sertoli cells, they can no longer survive and will eventually undergo apoptosis after DBP (present study), MEHP or other Sertoli cells toxicants treatment (Richburg and Boekelheide, 1996; Tay et al., 2007), increased temperature (cryptorchidism) (Wang et al., 2002; Kopecky et al., 2005), and hormonal withdrawal (Show et al., 2003). However, it remains unclear, in all the instances, whether the loss of vimentin filaments structure is a cause of spermatogenic cell apoptosis after testicular toxicant insult, or is a secondary effect resulting from loss of spermatogenic cell adhesion that occurs by other undefined mechanism.

Caspases are key mediators of apoptosis. Two major pathways (intrinsic and extrinsic) are involved in the process of caspase activation and apoptosis in mammalian cells. The intrinsic pathway for apoptosis involves the release of cytochrome c from mitochondria, then auto-activation of initiator caspase-9, and subsequently proteolytic activity of executioner caspase-3, -6, and -7 (Cecconi, 1999; Hengartner, 2000; Newmeyer and Ferguson-Miller, 2003). The extrinsic pathway for apoptosis involves the binding of a death receptor (Fas), to its ligand, FasL (Krammer, 2000; Algeciras-Schimnich et al., 2002). The binding of FasL to Fas induces the recruitment of initiator caspase-8 or -10 via a series of interactions, and ultimately activates executioner caspase -3, -6, and -7 resulting in cellular disassembly (Hengartner, 2000; Krammer, 2000; Algeciras-Schimnich et al., 2002). Both pathways converge on effector caspase-3, -7, and -6, which drive the terminal events of apoptosis. Byun et al. (2001) showed *in vitro* that apoptosis induced by truncated/collapsed vimentin is dependent on caspases activity, notably effector caspases 3, 6, and 7, and they also reported that caspases inhibitors antagonize truncated vimentin-induced apoptosis. In addition, truncated vimentin has also been shown to be a substrate for proteolytic cleavage by the initiator caspase 9 (Nakanishi et al., 2001). Similarly, in Jurkat cells stably transfected with a caspase-resistant vimentin, the onset of condensation or fragmentation of nuclei delayed during apoptosis induced by Fas activation (Morishima, 1999), and this stable cell line showed resistance to apoptosis induced by oxidative stress (Belichenko et al., 2001). These results suggest that truncated vimentin may play a role in the apoptotic process as a prerequisite for morphological change. Participation of Fas system (Lee et al., 1997; Richburg et al., 1999) and cleaved caspases (Bissonnette et al., 2008) were observed in phthalates-induced apoptosis. Moreover, in the present study, we have also observed reduction of actin staining intensity after DBP treatment. It has been reported earlier that caspase cleavage disrupts actin filaments and directly promotes apoptosis (Brancolini et al., 1995; Kothakota et al., 1997). Thus, it seems that activation of caspases and/or Fas/FasL may cause truncation of Sertoli cell vimentin filaments or vise-versa, and subsequently may induce spermatogenic cell apoptosis after DBP administration to prepubertal rats. However, this does not preclude the possibility of other mechanism for this phenomenon. The observations

reported in this study may provide insights into the mechanisms that regulate spermatogenic cell apoptosis in toxicant-induced testicular injury.

Acknowledgements

This work was supported in part by Grants-in-Aid from the Ministry of Education, Culture, Sports, Science and Technology of Japan (to M. Kurohmaru).

Conflict of interest statement

None of the authors has a conflict of interest.

References

Alam, M. S., S. Ohsako, T. Matsuwaki, B. X. Zhu, N. Tsunekawa, Y. Kanai, H. Sone, C. Tohyama, and M. Kurohmaru, 2010: Induction of spermatogenic cell apoptosis in prepubertal rats testes irrespective of testicular steroidogenesis: a possible estrogenic effect of di(n-butyl) phthalate. Reproduction. **139**, 427–437.

Algeciras-Schimnich, A., L. Shen, B. C. Barnhart, A. E. Murmann, J. K. Burkhardt, and M. E. Peter, 2002: Molecular ordering of the initial signaling events of CD95. Mol. Cell. Biol. **22**, 207–220.

Allard, E. K., K. J. Johnson, and K. Boekelheide, 1993: Colchicine disrupts the cytoskeleton of rat testis seminiferous epithelium in a stage dependent manner. Biol. Reprod. **48**, 143–153.

Amlani, S., and A. W. Vogl, 1988: Changes in the distribution of microtubules and intermediate filaments in mammalian Sertoli cells during spermatogenesis. Anat. Rec. **220**, 143–160.

Aumuller, G., M. Steinbruck, W. Krause, and H. J. Wagner, 1988: Distribution of vimentin-type intermediate filaments in Sertoli cells of the human testis, normal and pathologic. Anat. Embryol. **172**, 129–136.

Aumuller, G., C. Schulze, and C. Viebahn, 1992: Intermediate filaments in Sertoli cells. Microsc. Res. Tech. **20**, 50–72.

Belichenko, I., M. Morishima, and D. Separovic, 2001: Caspase-resistant vimentin suppresses apoptosis after photodynamic treatment with a silicon phthalocyanine in Jurkat cells. Arch. Biochem. Biophys. **390**, 57–63.

Bissonnette, S. L., J. E. Teague, D. H. Sherr, and J. J. Schlezinger, 2008: An endogenous prostaglandin enhances environmental phthalate-induced apoptosis in bone marrow B cells: activation of distinct but overlapping pathways. J. Immunol. **181**, 1728–1736.

Boekelheide, K., 1993: Cell toxicants. In: The Sertoli Cell (L. D. Russell and M. D. Griswold eds). Florida: Cache River Press, pp. 551–575.

Boekelheide, K., K. K. Johnson, and J. H. Richburg, 2005: Sertoli cell toxicants. In: Sertoli Cell Biology (M. K. Skinner and M. D. Griswold eds). San Diego: Elsevier Academic Press, pp. 345–382.

Brancolini, C., M. Benedetti, and C. Schneider, 1995: Microfilament reorganization during apoptosis: the role of Gas2, a possible substrate for ICE-like proteases. EMBO J. **14**, 5179–5190.

Byun, Y., F. Chen, R. Chang, M. Trivedi, K. J. Green, and V. L. Cryns, 2001: Caspase cleavage of vimentin disrupts intermediate filaments and promotes apoptosis. Cell Death Differ. **8**, 443–450.

Cecconi, F., 1999: Apaf1 and the apoptotic machinery. Cell Death Differ. **6**, 1087–1098.

Creasy, D. M., J. R. Foster, and P. M. Foster, 1983: The morphological development of di-N-pentyl phthalate induced testicular atrophy in the rat. J. Pathol. **139**, 309–321.

Creasy, D. M., L. M. Beech, T. J. B. Gray, and W. H. Butler, 1987: The ultrastructural effects of di-n-pentyl phthalate on the testis of the mature rat. Exp. Mol. Pathol. **46**, 357–371.

Dalgaard, M., A. Hossaini, K. S. Hougaard, U. Hass, and O. Ladefoged, 2001: Developmental toxicity of toluence in male rats: effects on semen quality, testis morphology, and apoptotic neurogeneration. Arch. Toxicol. **75**, 103–109.

Dostal, L. A., R. E. Chapin, S. A. Stefanski, M. W. Harris, and B. A. Schwetz, 1987: Testicular toxicity and reduced Sertoli cell numbers in neonatal rats by di(2-ethylhexyl)phthalate and the recovery of fertility as adults. Toxicol. Appl. Pharmacol. **95**, 104–121.

Foster, P. M. D., J. R. Foster, M. W. Cook, L. V. Thomas, and S. D. Gangolli, 1982: Changes in ultrastructure and cytochemical localization of zinc in rat testis following the administration of di-n-pentyl phthalate. Toxicol. Appl. Pharmacol. **63**, 120–132.

Franke, W. W., C. Grund, and E. Schmid, 1979: Intermediate-sized filaments present in Sertoli cells are of the vimentin type. Eur. J. Cell Biol. **19**, 269–275.

Galdieri, M., E. Ziparo, F. Palombi, M. A. Russo, and M. Stefanini, 1981: Pure Sertoli cell cultures: a new model for the study of somatic-germ cell interactions. J. Androl. **2**, 249–254.

Grasso, P., J. J. Heindel, C. J. Powell, and L. E. . Reichert Jr, 1993: Effects of mono(2-ethylhexyl) phthalate, a testicular toxicant, on follicle-stimulating hormone binding to membranes from cultured rat Sertoli cells. Biol. Reprod. **48**, 454–459.

Gray, T. J. B., and J. A. Beamand, 1984: Effects of some phthalate esters and other testicular toxins on primary cultures of testicular cells. Food Chem. Toxicol. **22**, 123–131.

Hall, E. S., J. Eveleth, and K. Boekelheide, 1991: 2,5-Hexanedione exposure alters the rat Sertoli cell cytoskeleton. II. Intermediate filaments and actin. Toxicol. Appl. Pharmacol. **111**, 443–453.

Heindel, J. J., and R. E. Chapin, 1989: Inhibition of FSH-stimulated cAMP accumulation by mono(2-ethylhexyl) phthalate in primary rat Sertoli cell cultures. Toxicol. Appl. Pharmacol. **97**, 377–385.

